NRL Report 6980

Electrical Noise in GaAs Diode Lasers

T. R. Royt

Emitter Location Branch
Electronic Warfare Division

October 30, 1969

NAVAL RESEARCH LABORATORY
Washington, D.C.

This document has been approved for public release and sale; its distribution is unlimited.

This report is based on the work leading to a thesis and is being issued as a final report on one phase of NRL Problem R06-38, Project SS33-18-11917.

ABSTRACT

This investigation makes measurements of the current fluctuations at 30 MHz generated in a GaAs diode during luminescent and lasing operation. For the diodes employed, it is found that thermal noise predominates over other effects. Calculations indicate that this dominance is due to the small junction resistances which occur at helium temperatures. In addition, the line loss in the transmission system was found to limit the measurement system sensitivity.

ACKNOWLEDGEMENT

The author wishes to express his appreciation for the many enthusiastic and imaginative discussions with Professor A. C. Scott of the University of Wisconsin, which stand as a source of direction and motivation.

Special thanks are also extended to R. A. Carpenter of the Naval Research Laboratory for his help in obtaining apparatus used in this investigation.

Finally, the author is indebted to Professor Hartmut Haug also of the University of Wisconsin who pointed out this problem after completion of his theoretical analysis.

Manuscript submitted September 2, 1969.

TABLE OF CONTENTS

	Page
ABSTRACT	i
ACKNOWLEDGEMENT	i
TABLE OF CONTENTS	ii
LIST OF ILLUSTRATIONS	iv
LIST OF SYMBOLS	vi
CHAPTER 1 – INTRODUCTION	1
CHAPTER 2 – NOISE THEORY	3
2.1 Basic concepts	3
2.2 Semiconductor diodes	9
2.3 Effects of lasing	10
CHAPTER 3 – RELATED INVESTIGATIONS	13
3.1 Si diodes	13
3.2 GaAs laser diodes	15
CHAPTER 4 – INVESTIGATION METHODOLOGY	17
4.1 Noise measurement	17
4.2 Dewar assembly	21
4.3 Noise transmission	25
4.4 Impedance transformation	29
CHAPTER 5 – DATA ANALYSIS	31
5.1 Presentation of results	31
5.2 Interpretation of results	36
CHAPTER 6 – CONCLUSIONS	37
ADDENDUM	39
APPENDIX A	40

TABLE OF CONTENTS – Continued

	Page
APPENDIX B	47
APPENDIX C	51
REFERENCES	54

LIST OF ILLUSTRATIONS

Figure	Title	Page
2.1.1	Thermal noise current equivalent circuit	6
2.1.2	Thermal noise voltage equivalent circuit	7
2.1.3	Semiconductor diode low current noise equivalent circuit	9
3.1.1	Low frequency noise measuring system as per Strutt	14
3.2.1	Light intensity fluctuation as a function of injection current in the lasing mode as per Armstrong	15
3.2.2	Light intensity fluctuation as a function of injection current in luminescent and lasing modes as per Armstrong	15
3.2.3	Current noise as a function of injection current as per Strutt	16
4.1.1	System schematic	18
4.1.2	System photograph	19
4.1.3	Ideal diode noise source	19
4.1.4	Amplifier video and subtractor outputs	20
4.1.5	System equipment photograph	21
4.2.1	Coldfinger assembly	23
4.2.2	Dewar assembly	24
4.2.3	Liquid helium level indicator	25
4.3.1	Noise transmission system schematic	25
4.3.2	Ideal noise transmission schematic	26
4.3.3	Current equivalent noise transmission schematic	26
5.1.1	Ideal low current diode noise equivalent circuits	31
5.1.2	Measured noise current as a function of injection current	34
5.1.3	Related noise current data as a function of injection current	35
A.1	Laser test system schematic	41
A.2	Subthreshold laser short pulsed	42
A.3	Above threshold laser short pulsed	43
A.4	Subthreshold laser long pulsed	44
A.5	Above threshold laser long pulsed	45

LIST OF ILLUSTRATIONS – Continued

Figure	Title	Page
B.1	Stub-tuned transformer	48
B.2	Transformer response, 540Ω:50Ω	49
B.3	Amplifier response	49
B.4	Transformer-amplifier response	50

LIST OF SYMBOLS

1. f Frequency
2. E Energy
3. $P(E)$ Probability
4. N No. of electrons per unit volume
5. K Boltzmann's constant
6. T Temperature
7. E_x Kinetic energy for the x degree of freedom
8. v_x Velocity in x direction
9. L Length of device
10. e Electronic charge
11. i_e Current due to one electron
12. τ_1 Thermal relaxation time
13. n Total No. of electrons
14. μ Mobility
15. A Cross sectional area of a device
16. r Resistance
17. g Conductance
18. ω Angular frequency
19. u, u' Independent dummy variables for t
20. s Dummy variable for τ
21. T_0 Integration time
22. i Current
23. I Fourier component of i
24. P_{ab} Power from a to b
25. τ_2 Recombination time
26. Δf Frequency interval
27. δi Instantaneous deviation of i(t) from the mean
28. $c(\tau)$ Autocorrelation coefficient
29. I_d Diode injection current
30. τ_3 Transit time between contacts
31. δN Instantaneous deviation of the carriers per unit volume from the mean
32. i_j Fluctuation current generated in the junction
33. i_s Fluctuation current generated in the bulk resistance
34. e_s Fluctuation voltage generated in the bulk series resistance
35. g_j, r_j Junction conductance and resistance
36. g_s, r_s Bulk conductance and resistance
37. I_0 Reverse saturation current
38. τ_p Hole lifetime
39. R_p Pump rate
40. R_{sp} Rate of spontaneous down transitions in all but the lasing mode
41. E_{cv} Rate of spontaneous down transitions in lasing mode

42. $\bar{n}$ Number of thermal and spontaneously emitted photons in the lasing mode
43. n_{th} No. of thermal photons
44. H Optical gain
45. κ Optical losses
46. n_{sp} Spontaneously emitted photons
47. $K(n)$ Population noise due to light field fluctuations
48. b Constant
49. T_{He} Temperature due to liquid helium cooling
50. G Electrical gain
51. i_{dT} Total equivalent diode fluctuation current
52. Z_0 Characteristic line impedance
53. Z_L Load impedance
54. r_d Total equivalent diode resistance
55. Z_s Transmission line input impedance at diode end
56. l Line length
57. ρ_L Reflection coefficient at load
58. i_L Current into load
59. i_s Current into line at diode end
60. β Propagation constant
61. r_r Reference source impedance
62. i_r Reference fluctuation current
63. P_{Ld} Power in load due to diode
64. P_{Lr} Power in load due to reference source
65. α Line attenuation constant
66. l_d Length of line from diode
67. l_r Length of line from reference source
68. T_{290} 290°K
69. T_{77} 77.3°K
70. $l_{1/4\lambda}$ Length of quarter wave line
71. A_{dl} Attenuation in a quarter wave line
72. $\rho^{l}_{1/4\lambda}$ Reflection coefficient of a quarter wave line at the end opposite to a short
73. $\rho^{t}_{1/4\lambda}$ Reflection coefficient of a quarter wave line at the end opposite to the diode load
74. $\rho^{d}_{0\lambda}$ Reflection coefficient at the diode load
75. $Z^{l}_{1/4\lambda}$ Impedance measured on a quarter wave line at the end opposite to a short
76. $Z^{t}_{1/4\lambda}$ Impedance measured on a quarter wave line at the end opposite to the diode load

CHAPTER 1

Introduction

Shortly after the appearance in the early 1950's of the transistor and the associated pn junction analyses, experimental investigations into the associated noise spectra were reported.[1] Still other papers followed during the middle and late 1950's which contained data from noise experiments on semiconductor diodes of various compositions, and which also postulated electrical models and mathematical methods to explain the empirical relationships which resulted from this data.[2,3,4,5,6,7]

With the development of the GaAs injection diode laser in 1962, the old semiconductor diode noise problem evolved to a somewhat more complex form.[8] The first papers to concern themselves with a noise analysis per se of this more interesting problem, appeared in 1964.[9,10,11] These papers dealt with the fluctuations of the light field and did not address themselves to an analysis of the electrical noise. Some attempt was made at this latter problem in 1967 and 1968.[12,13] These reports, however, were confined to operation well below threshold and to low frequencies. It remained for Haug in 1967 to set forth a theoretical treatment of high frequency electrical noise in the GaAs diode laser from a quantum mechanical point of view.[14] In this report, a diode model was postulated and a theoretical expression describing the primary noise components in the luminescent and lasing modes was developed with particular emphasis on the transition through threshold. There was at this time, however, no experimental analysis of the electrical noise in the GaAs diode laser.

The research reported in this report was begun in order to fill this gap in the otherwise comprehensive reporting of experimental noise investigations in materials and electrical devices. Several months after commencing this investigation, a paper by G. Guekos and M. J. O. Strutt appeared which reported experimental results of noise measurements on luminescent GaAs diodes.[13] These results were restricted not only to luminescent modes but also to low current densities and to frequencies below 1.5 MHz. In contrast, the work reported in this report concentrates on an analysis of the region around threshold. It is at threshold that the feature distinguishing the laser diode from any ordinary pn junction

becomes most evident. And since this unique generation-recombination process should imply in particular a distinct shot noise relationship, it is only natural to expect shot noise in the region of threshold to be the singular phenomenon of interest in the GaAs diode laser.

In Chapter 2 the basis will be established for the approach used in making the noise measurements and for the physical explanation of the resulting relationships. In addition to elementary noise theory, the application of this theory to semiconductor diodes and the interesting change in the noise properties due to spontaneous and stimulated emission in the junction region are the topics of discussion.

The third chapter contains a review of other experimental investigations. An attempt is made to relate the theory of Chapter 2 to the results of these investigations in order to seek out implications which are relevant to the investigation at hand. This facilitates both the selection of measurement techniques and the interpretation of results, problems which are treated in Chapters 4 and 5.

In the fourth chapter is contained the procedure used to measure the noise in the GaAs diode lasers. Noise measuring techniques have been around for some time and it is easy to take a cursory glance at the problem here and believe it to be a trivial one. But such is not the case. Therefore, an extensive analysis of the problems unique to this investigation is given here with the considerations which lead to some very interesting solutions.

The recorded data and associated relationships are presented in Chapter 5. This information is then interpreted in light of the theory now at our disposal and other experimental investigations. And finally in the sixth chapter the basic structure of the investigation and observations on results, theory, and techniques, made during the investigation, are summarized.

CHAPTER 2

Noise Theory

In this chapter a discussion of the theory for a noise analysis of the laser and the measuring system is undertaken. It will be shown that the statistical processes of the laser yield to a Fourier analysis. The resulting mathematical expression for noise is then transformed into an electrical circuit representation for manipulation. Since the measuring system noise parameters are expressed in the same representation as those for the laser, it will be possible to get some feeling for the requirements to be placed upon the measuring system from the standpoint of sensitivity, selectivity, and compatability with the laser. That these methods are approximations, whose degrees of validity are contingent upon the choice of a model, cannot be overemphasized. And it is for this reason that this chapter has been titled noise theory, reserving the discussion of the application of these models to physical devices for later chapters.

2.1 Basic concepts

That excess noise is characterized by a 1/f spectrum was one reason for performing this investigation at fairly high frequencies, and consequently obviates any need to consider such noise here. This leaves thermal and shot noise as the remaining components of interest in a semiconductor. While shot noise per se occurs in conjunction with transport phenomena, thermal noise is more basic. Thermal noise may be evidenced in any physical process and is caused by the inherent thermal energy of the participating particles. It is normally assumed that the probability that a conduction electron has kinetic energy, E, is given by the Maxwell distribution,

$$P(E) = 2N\left(\frac{E}{\pi(kT)^3}\right)^{1/2} e^{-E/KT} \tag{2.1.1}$$

such that $\overline{E} = 3KT/2$. Then by equipartition of energy between degrees of freedom, $\overline{E}_x = \frac{1}{2}m\overline{v_x} = \frac{1}{2}KT$. And it is this mean velocity per electron, directed along mean free

paths which are colinear with an axis connecting the device contacts, which is responsible for the stationary random current fluctuations.

An expression for the mean square of the fluctuations will be developed by finding their autocorrelation function and then by applying a Fourier analysis to this. To begin, it must be recognized that an electron moving at v_x will cause an instantaneous current ev_x/L such that $i_e(t) = \sum_m \frac{e}{L} v_{xm}(t)$, giving the current due to a single electron as its velocity changes magnitude during m statistically occurring collisions.[15] Assuming that current pulses separated by collisions are not correlated, there results the autocovariance function

$$\overline{i_e(t)\, i_e(t+\tau)} = \left(\frac{e}{L}\right)^2 \overline{v_{xm}^2}\, e^{-\tau/\tau_1} = \left(\frac{e}{L}\right)^2 \frac{KT}{m} e^{-\tau/\tau_1}, \tag{2.1.2}$$

where correlation exists only in so far as $e^{-\tau/\tau_1}$ is the probability that there occurs no collision during τ. Now, since the electrons interact primarily with the lattice, we neglect lattice vibration and maintain that

$$\overline{\sum_n i_{en}(t)\, i_{en}(t+\tau)} = \sum_n \overline{i_{en}(t)\, i_{en}(t+\tau)} \tag{2.1.3}$$

or that the pulses from all n electrons during τ are uncorrelated. This allows one to write

$$\overline{i(t)\, i(t+\tau)} = n\left(\frac{e}{L}\right)^2 \frac{KT}{m} e^{-\tau/\tau_1} \tag{2.1.4}$$

or since $\frac{1}{r} = g = \frac{A}{L}\frac{\mu ne}{AL} = \frac{ne^2\tau_1}{L^2 m}$,

$$\overline{i(t)\, i(t+\tau)} = \frac{gKT}{\tau_1} e^{-\tau/\tau_1} \tag{2.1.5}$$

Because i(t) is stationary, $\overline{i(t)\, i(t+\tau)} = \overline{i(t)\, i(t-\tau)}$. The autocorrelation function, 2.1.5, becomes very useful as a short digression into the Fourier analysis of fluctuating quantities will show.

As it will be desirable to convert later to a circuit representation, in order that the noise theory will be compatable with system parameters, it is only natural that one should go to frequency space for expedient handling of system transfer functions. Therefore, consider a time dependent fluctuation x(t) over $0 \le t \le T_0$

$$x(t) = \sum_{n=-\infty}^{\infty} a_n e^{j\omega_n t} \tag{2.1.6}$$

where $\omega_n = \dfrac{2\pi n}{T_0} = n\Delta\omega$

$$a_n = \frac{1}{T_0}\int_0^{T_0} x(u)e^{-j\omega_n u}\, du$$

A particular Fourier component is

$$X(\omega_n) = a_n e^{j\omega_n t} + a_n^* e^{-j\omega_n t}$$

$$= 2|a_n| \cos(\omega_n t + \phi_n) \tag{2.1.7}$$

And its mean square is given by

$$\overline{X^2(\omega_n)} = \overline{2a_n a_n^* e^{j(\omega_n t - \omega_n t)}} = \overline{2a_n a_n^*}$$

$$= \frac{2}{T_0^2}\overline{\int_0^{T_0}\int_0^{T_0} x(u)\, x(u')\, e^{-j\omega_n(u-u')}\, du\, du'}$$

$$= \frac{2}{T_0^2}\int_0^{T_0} du \int_{-u}^{T_0-u} \overline{x(u)\, x(u+s)}\, e^{j\omega_n s}\, ds$$

$$= \frac{2}{T_0^2}\int_0^{T_0} du \int_{-\delta}^{+\delta} \overline{x(u)\, x(u+s)}\, e^{j\omega_n s}\, ds \tag{2.1.8}$$

where $T_0 \gg \tau_1$, the relaxation time for the fluctuations, and where δ is related to τ_1 such that $\delta \ll T_0$. Thus with $\overline{x(u)\, x(u+s)}$ independent of u one may write

$$\overline{X^2(\omega_n)} = 4\Delta f \int_0^{\infty} \overline{x(u)\, x(u+s)}\, e^{j\omega_n s}\, ds \tag{2.1.9}$$

If one considers frequencies such that $\omega_n \tau_1 \ll 1$ we then have, putting u = t and letting $T_0 \to \infty$,

$$\frac{\overline{X^2(\omega)}}{df} = 4\int_0^{\infty} \overline{x(t)\, x(t+s)}\, ds \tag{2.1.10}$$

which is the Wiener-Khintchine theorem.

Using theorem 2.1.10, the relationship for the frequency spectrum of the current fluctuations is found by substituting 2.1.5 into 2.1.10 such that

$$\frac{\overline{I^2(\omega)}}{df} = 4KTg\frac{1}{\tau_1}\int_0^\infty e^{-\tau/\tau_1}\,d\tau \tag{2.1.11}$$

$$= 4KTg$$

And we have the expression characterizing thermal current fluctuations in frequency space for a semiconductor or metal having temperature T and resistance $r = 1/g$. Converting to power representation, the frequency independent expression 2.1.11 is integrated over Δf to get

$$\overline{i^2} = 4KTg\ \Delta f. \tag{2.1.12}$$

Finally it is necessary to convert the mathematical expression for the current fluctuations into electrical representation so that it may be manipulated for system analysis. It is apparent that a current of $i = (4KTg\ \Delta f)^{1/2}$ would flow through a short circuit across the device. If instead, a resistance $r_2 = 1/g_2$ is placed in parallel with the device under consideration, which we assume is purely resistive at $r_1 = 1/g_1$, it is the case that the current must divide between the device and g_2. The component of fluctuating current through g_2 causes a power dissipation in g_2 of

$$P_{12} = 4KTg_1\,\Delta f\left(\frac{g_2}{g_1 + g_2}\right)^2\frac{1}{g_2} \tag{2.1.13}$$

over a spectral region of Δf. If $g_1 = g_2$ we have that $P_{12} = KT\ \Delta f$, commonly refered to as the available noise power of g_1. It is important to point out that since g_2 is also a device at temperature, T, and as a consequence of the second law of thermodynamics,

$$P_{21} = 4KTg_2\,\Delta f\left(\frac{g_1}{g_1 + g_2}\right)^2\frac{1}{g_1} = P_{12}. \tag{2.1.14}$$

Thus, it is seen that expression for current fluctuations yields easily to a circuit representation, where the device is described by an ideal current source in parallel with a noiseless resistance equal to that of the device.

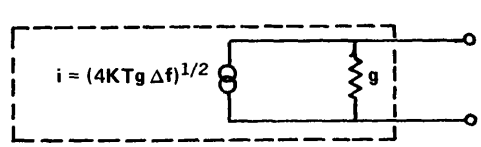

Fig. 2.1.1 – Thermal noise current equivalent circuit

With this equivalence established, Thevenin's theorem may be used to represent the device as shown below.

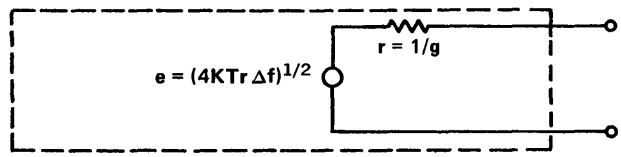

Fig. 2.1.2 – Thermal noise voltage equivalent circuit

Furthermore if two resistances are in parallel, their combined noise current fluctuations are simply represented by a current generator, $i = [4KT(g_1 + g_2)\,\Delta f]^{1/2}$, shunted with the parallel combination of g_1 and g_2.

Having briefly touched on the theory of thermal noise, we turn to a discussion of something perhaps somewhat more germane to this investigation, the theory of shot noise. If use is made of the Wiener-Khintchine theorem, 2.1.10, already developed during the discussion of thermal noise, it remains necessary only to derive an expression for the autocorrelation function, $\overline{x(t)\,x(t+\tau)}$, for shot noise. Since the transport process which is responsible for the shot noise involves both a statistical and a mean current, the current fluctuations are represented by $\delta i(t)$ where $\delta i(t) \equiv i(t) - \overline{i(t)}$. Thus the autocorrelation to be defined is

$$\overline{\delta i(t)\;\delta i(t+\tau)} = \overline{\delta i^2(t)}\,c(\tau) \tag{2.1.15}$$

where $c(\tau)$ is, again, the autocorrelation coefficient, this time given by $c(\tau) = e^{-\tau/\tau_2}$. Note that τ_2 is the mean lifetime of a carrier before it recombines. It now becomes extremely important to define the physical process for which the autocorrelation function is to be developed, for there are important implications which relate to this investigation.

If the shot noise created in the neutral bulk region of a semiconductor diode is considered, it is seen, from the same viewpoint taken in the thermal analysis, that

$$\delta i(t) = [N(t) - \overline{N(t)}]\frac{ev_{xd}}{L} = [N(t) - \overline{N(t)}]\frac{e}{\tau_3} \tag{2.1.16}$$

where v_{xd} is the drift velocity, τ_3 the lifetime, and L the length of the bulk region. It follows that

$$\overline{\delta i^2(t)} = \overline{[N(t) - \overline{N(t)}]^2}\left(\frac{e}{\tau_3}\right)^2. \tag{2.1.17}$$

And assuming that the carriers obey a Poisson distribution, giving $\overline{[N(t) - \overline{N(t)}]^2} = \overline{N(t)}$, we have

$$\overline{\delta i^2(t)} = \overline{N(t)}\left(\frac{e}{\tau_3}\right)^2. \tag{2.1.18}$$

Substituting $\overline{i(t)} = e\overline{N}/\tau_3 = I_d$, we finally have

$$\overline{\delta i^2(t)} = \frac{I_d e}{\tau_3}. \tag{2.1.19}$$

The desired frequency spectrum follows immediately from 2.1.10, 2.1.15, and 2.1.19 as,

$$\frac{\overline{\delta I^2(\omega)}}{df} = 4\int_0^\infty \frac{I_d e}{\tau_3} e^{-\tau/\tau_2}\, d\tau$$

$$= 4eI_d\frac{\tau_2}{\tau_3} \tag{2.1.20}$$

for $\omega\tau_3 \ll 1$.

Another source of shot noise, and one of considerable importance to this investigation, is the pn junction of a semiconductor diode. Letting τ_2 be the mean time of recombination for the excess minority carriers, we confine the noise model to a narrow region about the junction, and describe the current fluctuation here by

$$\delta i(t) = [N(t) - \overline{N(t)}]\frac{e}{\tau_2}. \tag{2.1.21}$$

Thus

$$\overline{\delta i^2(t)} = \overline{[N(t) - \overline{N(t)}]^2}\left(\frac{e}{\tau_2}\right)^2 = \overline{\delta N^2(t)}\left(\frac{e}{\tau_2}\right)^2. \tag{2.1.22}$$

Since $\overline{\delta N^2(t)} = \frac{\tau_2}{2}(2R)$ and $I_d = eR$,

$$\frac{\overline{\delta I^2(t)}}{df} = 4\int_0^\infty \frac{I_d e}{2\tau_1} e^{-\tau/\tau_1}\, d\tau$$

$$= 2eI_d \tag{2.1.23}$$

The much larger magnitude of the junction shot noise relative to bulk shot noise allows us to neglect the latter in a circuit representation. The current fluctuations may be represented as an ideal current source of $i_j = (2eI_d\ \Delta f)^{1/2}$ in parallel with the junction conductance, $g_j = e(I_d + I_0)/KT$, and all of this in series with the bulk resistance and its equivalent thermal noise generator as in Fig. 2.1.3. It is noteworthy that this final result

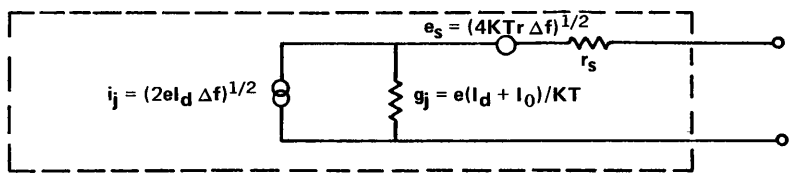

Fig. 2.1.3 – Semiconductor diode low current noise equivalent circuit

is obtained only for the special transport processes assumed here. Indeed, as we shall see, if this relation were physically inviolable, this investigation would have been pointless.

2.2 Semiconductor diodes

In 1955 there appeared one of the first papers to concern itself with shot noise in junction diodes.[3] In this work Van der Ziel applied transmission line theory, whose equations of motion are nearly identical to those for diffusion processes, to the development of an expression for the shot noise caused by a pn junction. Assuming a slightly more specific model but of the same general configuration as was considered in the previous section, Van der Ziel derives a form of the Wiener Khintchine theorem similar in essential features to the relation in section 2.1. In fact, at low frequencies and high forward current, Van der Ziel's relation assumes the identical form of the other. The final result is given as

$$\overline{\delta i_j^2(t)} = 4KTg_j\ \Delta f - 2eI_d\ \Delta f \tag{2.2.1}$$

where $g_j = \frac{e}{KT}(I_d + I_0)\left[\frac{1}{2}(1 + \omega^2\tau_p^2)^{1/2} + \frac{1}{2}\right]^{1/2}$. Shortly thereafter an interpretation by Uhlir[4] was expanded by Van der Ziel[6] to account for the above results in terms of the

general analysis which resulted in equation 2.1.23. To do this, the diode current was simply broken down into three components.

(1) Carriers crossing the transition region and then recombining.

(2) Carriers crossing the transition region from the opposite direction and then recombining.

(3) Carriers crossing the transition region and, then, through thermal effects, crossing back again before recombining.

Summing the shot noise resulting from each of these, there results

$$\overline{\delta i_j^2(t)} = 2e(I_d + I_0)\,\Delta f + 2eI_0\,\Delta f + 4KT(g - g_0)\,\Delta f. \tag{2.2.2}$$

Since $g_0 = e(I_d + I_0)/KT$, substitution yields

$$\overline{\delta i_j^2(t)} = 4KTg_j\,\Delta f - 2eI_d\,\Delta f. \tag{2.2.3}$$

It should be noted that the above theories have assumed low injected minority carrier density such that the carrier crossings are independent of one another. If high current is passed through the diode, the voltage across the depletion region is dependent on the resulting high density of excess carriers. Since this voltage influences the number of carriers crossing the junction, the carrier crossings are obviously not independent. And it is speculated that the $2eI_d$ component may decrease at high currents giving a net increase in the shot noise, a very important consideration in view of Fig. 2.1.3.

2.3 Effects of lasing

It is reasonable to presume that the presence of a light field which interacts with the carriers of a diode should still further complicate the noise model. The problem is approached generally by deriving an expression for the autocorrelation function, $\overline{\delta i_j(t)\,\delta i_j(t+\tau)}$. As $\overline{\delta i_j(t)\,\delta i_j(t+\tau)} = (e^2/\tau_2^2)\,\overline{\delta N(t)\,\delta N(t+\tau)}$ it is only necessary to find $\overline{\delta N^2(t)}$. This is done[14] by first writing the quantum mechanical Langevin equations for the operators of the light mode, the atomic dipole moments, and the population of a k state. Then a rate equation for the population of the conduction band consisting of a mean and a fluctuating part may be found. We thus get an equation for the fluctuating Fermi level which is solved below and above threshold. The result below threshold gives

$$\overline{\delta N^2(t)} = \frac{\tau_2}{2}\{R_{sp} + R_p + (\bar{n} + 1)\,E_{cv} + \bar{n}E_{vc}\}$$

$$+ 4 \frac{\tau_2 \cdot H^2}{\tau_2^{-1} + 2(\kappa - H)} \bar{n}(\bar{n} + 1)$$

$$+ 2 \frac{\tau_2 \cdot H}{\tau_c^{-1} + 2(\kappa - H)} \{(\bar{n} + 1) E_{cv} + \bar{n} E_{vc}\} \tag{2.3.1}$$

and that above threshold is

$$\overline{\delta N^2(t)} = \frac{\tau_2}{2}\{R_{sp} + R_p + (\bar{n} + 1) E_{cv} + \bar{n} E_{vc}\}$$

$$+ 2\bar{n} H_s^2 \frac{\tau_2^2 \tau_s^2}{\tau_2 + \tau_s}\{E_{cv} + E_{vc} + 4\kappa(n_{th} + 1/2)\}$$

$$+ 2\bar{n} H_s \frac{\tau_2^2 \tau_s}{\tau_2 + \tau_s}\{E_{cv} + E_{vc}\} \tag{2.3.2}$$

where $\tau_s^{-1} = \dfrac{2\alpha\bar{n}\kappa}{1 + \alpha\bar{n}}$ is the time constant of the light field intensity correlation function and where $\kappa = H(1 + \alpha\bar{n})^{-1}$.

As only the junction effects are of concern, the term R_p, which accounts for the pump from the terminals, is not included in the following development. Now, the junction current is given by

$$I_d = e\{R_{sp} + (\bar{n} + 1) E_{cv} - \bar{n} E_{vc}\}. \tag{2.3.3}$$

And making use of the Wiener Khintchine theorem,

$$\frac{\overline{I^2(\omega)}}{df} = 4 \int_0^\infty \overline{i_j(t)\, i_j(t + \tau)}\, d\tau$$

$$= 4 \frac{e^2}{\tau_2^2} \int_0^\infty \overline{\delta N(t)\, \delta N(t + \tau)}\, d\tau$$

$$= 4 \frac{e^2}{\tau_2^2} \int_0^\infty \overline{\delta N^2(t)}\, C(\tau)\, d\tau$$

$$= 4 \frac{e^2}{\tau_2^2} \overline{\delta N^2(t)} \int_0^\infty e^{-\tau/\tau_2}\, d\tau$$

$$= 4 \frac{e^2}{\tau_2} \overline{\delta N^2(t)} \tag{2.3.4}$$

It is now simply a matter of substitution of 2.3.1 or 2.3.2 into 2.3.4 and the replacement of $\frac{\tau_2}{2} R_{sp} + (\bar{n} + 1) E_{cv} + \bar{n}E_{vc}$ in 2.3.1 and 2.3.2 by $\frac{\tau_2 I_d}{2e} + 2\frac{\tau_2}{2}\bar{n}E_{vc}$ in order to arrive at

$$\frac{\overline{I^2(\omega)}}{df} = 4\frac{e^2}{\tau_2}\left\{\frac{\tau_2 I_d}{2e} + \tau_2 \bar{n}E_{vc} + K(\bar{n})\right\}$$

$$= 2eI_d + 4e^2\bar{n}E_{vc} + 4\frac{e^2}{\tau_2}K(\bar{n}) \qquad (2.3.5)$$

where $K(\bar{n})$ is the population noise due to the light field fluctuations. As Haug points out, $K(\bar{n})$ becomes very interesting near threshold. Rewriting the above equation, and retaining only the important terms, there results just below threshold

$$\frac{\overline{I^2(\omega)}}{df} = 2eI_d + \left(\frac{4en_{sp}H\kappa}{b(I_0 - I_d)}\right)^2\left\{\tau_2^{-1} + 2b(I_0 - I_d)\right\}^{-1} \qquad (2.3.6)$$

Since $\kappa - G = b(I_0 - I_d)$, the increase in the power spectrum attributed to $K(n)$ should increase near threshold as $(I_0 - I_d)^{-x}$, where x varies from 3 to 2 as τ_2^{-1} goes from $\tau_2^{-1} < 2(\kappa - G)$ to $\tau_2^{-1} > 2(\kappa - G)$. As the injection current increases and threshold is passed, that portion if $K(\bar{n})$ due to fluctuations in the light field intensity becomes constant because of saturation of the spontaneous emission into the light mode. The portion of $K(\bar{n})$ due to the correlation of the light field with population fluctuations increases linearly with $\bar{n}$ above threshold.

If $\bar{n}$ were to be very small, it is interesting to observe that the shot noise would be given as $2eI\,\Delta f$ just as expected. Thus, according to this theory, one should expect $2eI_d\,\Delta f$ to express the shot noise current fluctuations of this laser diode, changing to a quadratic increase with I_d as threshold is approached, and finally a reversion to the linear dependence on I_d above threshold.

CHAPTER 3

Related Investigations

In the preceding chapter, a general description of the noise characteristics of a semiconductor laser diode was presented. This description was comprised of many theories which for the most part were mutually supplemental. A number of the treatments were refinements of other models that were used only for a mathematical basis. That the actual description of the noise in a semiconductor laser diode is open to question, will receive further confirmation in this chapter. Here, related experimental work on diodes will be presented and compared to theory. Although the two will differ somewhat, some very general correlations will be noted.

Also of interest in this chapter are the techniques applied in acquisition of the noise data. Such background will be useful in formulating a measurement system for this investigation.

3.1 Si diodes

Schneider and Strutt, in 1959, published a fairly extensive treatment of Si diodes, the experimental work of which agreed quite well with the theory.[7] The measurement system was configured as shown in Fig. 3.1.1. The scheme is quite straight forward. A dc current source supplies the diode, and the noise current is coupled through a capacitor to the measuring system. The output of the system is noted for a particular diode current. A switch then disconnects the diode circuit and replaces it with a variable resistor, R_e. R_e is varied until the same system output results. These resistance measurements, although incorrectly referred to as equivalent resistances for the Si junction, are a measure of the noise current fluctuations of the diode.

A particularly important part of the measuring system, the transformer, deserves special attention. In coupling networks, maximum power transfer is always sought and is achieved by matching the output impedance of the first network to the input impedance of the second. But unique to this measurement system is another condition, that of

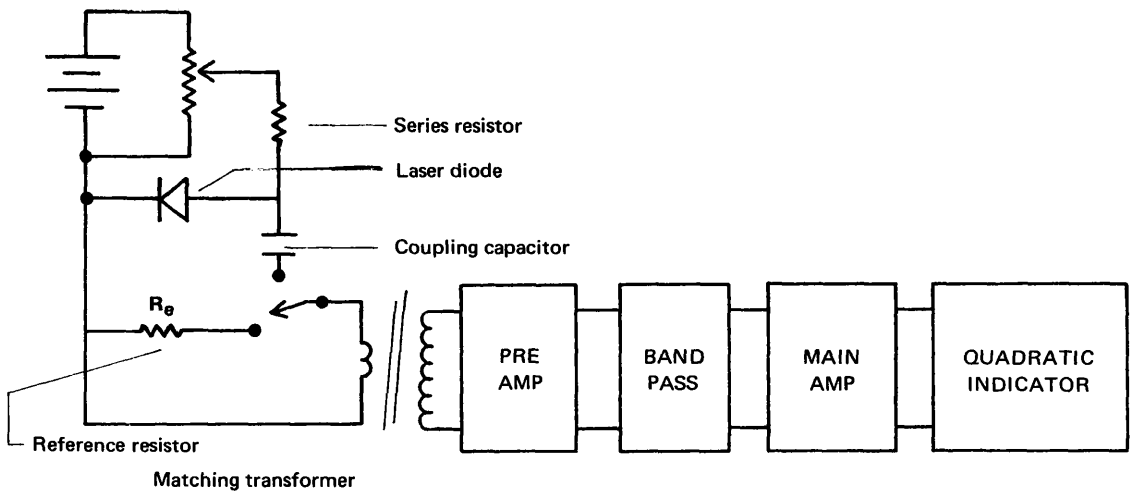

Fig. 3.1.1 – Low frequency noise measuring system as per Strutt

minimizing the noise figure of the amplification sections. Manipulation of a few noise figure-amplifier relationships shows that only the noise figure of the first stage of amplification is really of significance. It can be shown that as the output resistance, R_0, of the first network is varied from zero to infinity the noise figure goes through a minimum for

$$R_0 = \left\{ \frac{R_n R_1}{n_1} \right\}^{1/2},$$

where R_n = input noise resistance of the first tube

R_1 = parallel combination of the input tube resistance and the input circuit impedance

n_1 = noise ratio of R_1 (as the tube input impedance may have a noise ratio different from 1)

It is often the case that the R_0 for minimum noise figure is less than the R_0 for matched conditions by a factor of 5 or 10. In these cases a compromise match is necessary. In any case, because of the usually small impedances of the diodes to be analyzed, a transformer is required to attain the proper match, lest the amplified diode noise be covered by the inherent amplifier noise.

Probably the most interesting feature of the experimental results from our point of view is the substantial deviation of R_e from the predicted values, as the diode current was increased above 1 ma. These results are in agreement with the expectations for

high-level injection referred to in 2.2, thus affirming the lack of a good theoretical diode noise model for high current levels.

3.2 GaAs laser diodes

Probably the first experimental investigation into the noise properties of GaAs laser diodes was reported in late 1965 by Armstrong and Smith.[10,11] This work concerned itself only with the light field fluctuations. Although according to Haug the influence of the population fluctuations on the coherence properties of the laser light is very small, the results of this report are of interest in that effects of intensity fluctuations as well as population fluctuations will be evidenced in the current fluctuations to be measured in our investigation.

The relative intensity fluctuation for a lasing mode as a function of injection current is shown in Fig. 3.2.1. It is seen that at injection levels below but near a threshold of ~22.8 ma, the fluctuations increase with the injection current. As threshold is passed, the fluctuations tend to level off, and they finally decrease as injection levels exceed ~25% above threshold. Armstrong and Smith also measured the intensity fluctuations of nonlasing modes and their correlation with the lasing mode. As is evident from Fig. 3.2.2, one of the nonlasing modes is much more noisy than the lasing mode, especially after the threshold of the lasing mode is exceeded and its fluctuations are beginning to fall off. Interesting, too, is the correlation, ρ_{12}, between the lasing and nonlasing modes. These results once more raise the question of whether one can correlate theoretical models, such as that developed by Haug, with experimental work. In the work presented

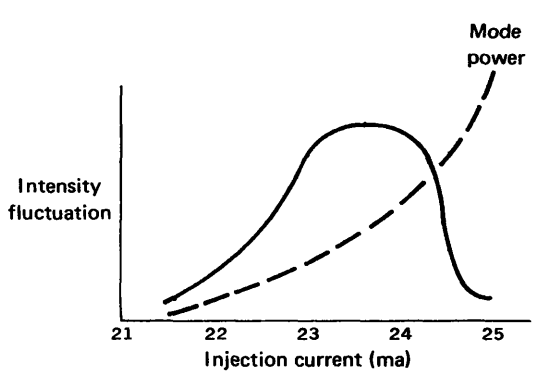

Fig. 3.2.1 – Light intensity fluctuation as a function of injection current in the lasing mode as per Armstrong

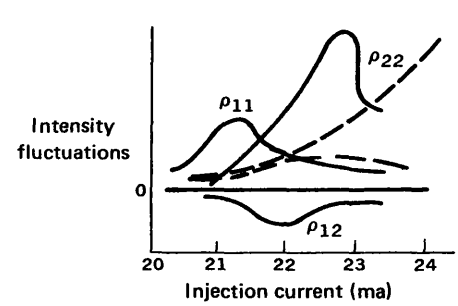

Fig. 3.2.2 – Light intensity fluctuation as a function of injection current in luminescent and lasing modes as per Armstrong

above, frequency discrimination techniques can be used, but the chances of attributing noise to a particular mode merely on the basis of an amplitude analysis of current fluctuations appear to be small. In any case, this further adds to the question of just what type of current fluctuation should one expect as a function of injection current.

In 1967, Brophy made the first investigation on GaAs diodes to concern itself with current fluctuations.[12] However, here again the results were restricted to light field fluctuations. Only that portion of the current fluctuations that was correlated with the light field fluctuations was recorded. It was found that 1/f noise dominated the measurements made on laser diodes operated well below threshold and at frequencies up to 10 kHz.

Shortly after the appearance of the theoretical paper by Haug, results of an experimental investigation on the current noise in the luminescent modes of GaAs laser diodes were published by Strutt.[13] The measuring system consisted of a high input impedance preamplifier followed by the main amplifier, filters, and a true rms voltmeter or heterodyne voltmeter. An analysis of 1/f noise showed that it tended to level off above 2 MHz, the highest frequency at which data were taken. As injection current was increased from 0.1 to 5 ma at 1.3 MHz, fluctuations for two luminescent laser diodes followed curves shown in Fig. 3.2.3. That these results exceeded 2eI shot noise by general orders of magnitude was extremely encouraging. It will be important, however, to remember that in this case with $I_d = 5$ ma and $T = 290°K$, $I_d = I_0(e^{eV/mkT} - 1)$, $m = 1$ to 2; therefore,

$$g_j = \frac{e}{mkT}(I_d + I_0) \cong \frac{e}{mkT} I_d$$

such that $g_j \approx 0.1$ mho or $r_j \approx 10$ ohms. It was thus interesting that this paper, even though a response to Haug's theory on effects around threshold, concerned itself only with currents well below threshold.

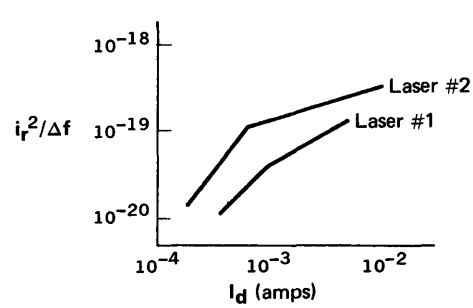

Fig. 3.2.3 – Current noise as a function of injection current as per Strutt

CHAPTER 4

Investigation Methodology

In the previous chapters salient features of noise theory and several experimental investigations, as they apply to the problem at hand, have been discussed. Not only is the magnitude of the shot noise expected from the diode open to question, but the relationship it bears to the injection current is uncertain. There was some reason to believe that the shot noise would be difficult to see if it went as pure $2eI_d$, since the junction resistance at low temperatures would be very small. But at the same time it was recognized that lasing and high injection effects might compensate for this. But in any case the results of the experiments in section 3.2 indicated that, even if the junction shot were dominant over the thermal noise, it would be necessary to perform this investigation at frequencies well enough above 1 or 2 MHz that 1/f effects would be of no consequence. Finally, it was evident that the internal noise of an amplifier could mask the diode shot noise if the necessary precautions were not taken.

With the preceding information as a base it will now be possible to design a noise measuring system suited to needs of this investigation. The problem of amplification of the noise to a level at which it can be operated on and the method of fitting this noise into a frame of reference will be discussed first. Constraints on the system resulting from laser operation, threshold detection, impedance determination, frequency of operation, line loss, mismatches, and band width considerations will then be successively discussed. During this discussion it will be convenient to refer to the system schematic in Fig. 4.1.1 and photograph, Fig. 4.1.2.

4.1 Noise measurement

Probably the most requisite element of the measuring system is the amplifier. It may be employed in the system in three basic configurations. As has been seen previously, one method is to connect the noise source to the input and to record the output. This method suffers from the difficulty in obtaining a large output due to noise from the device

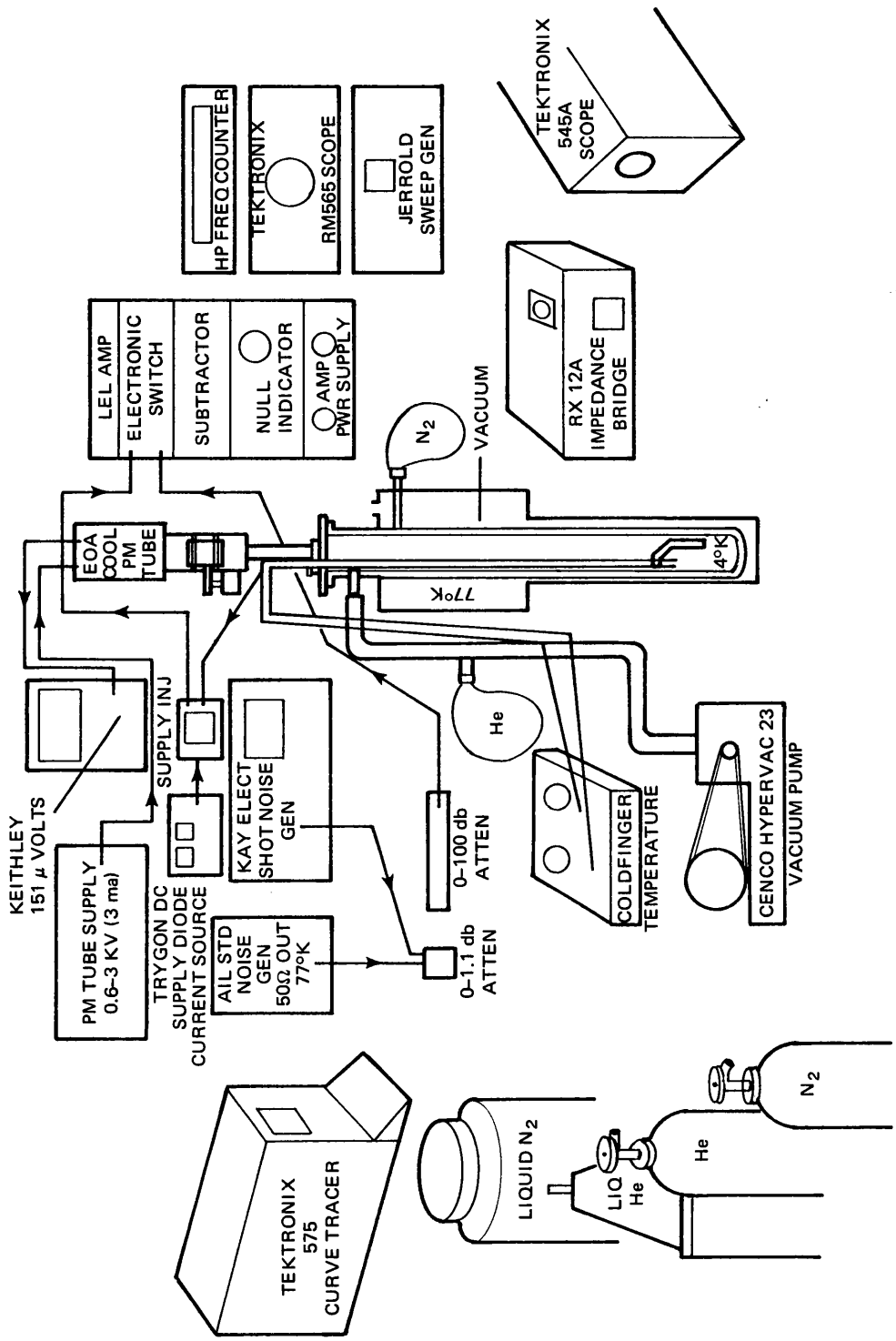

Fig. 4.1.1 – System schematic

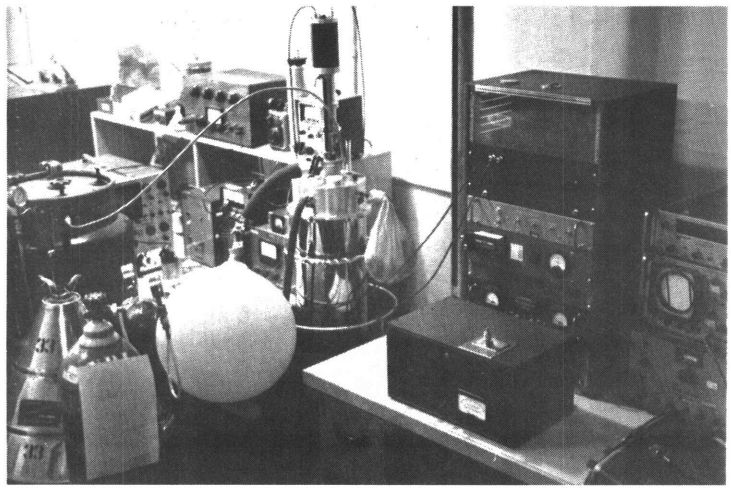

Noise measurement system (see Fig. 4.1.1 for identification)

Fig. 4.1.2 – System photograph

while preventing the recording device from being saturated by the amplified internal noise of the amplifier. The obvious solution is to use correlation techniques.[16] Such an alternate method involves the use of two amplifiers whose internal noises are of course uncorrelated. But a third technique, which only requires one amplifier and works nearly as well as the second, is to chop the amplifier input, shorting the input on every other sample, and then subtract the shorted chopped outputs from the unshorted ones. This is of course the principle used in the design of noise figure indicators.[17] The result is that depending on the accuracy of the subtraction electronics the noise figure of the amplifier is of much less consequence.

Common to all three of these techniques, however, is the need for amplification of the diode noise to a level where it is useful. Let it be assumed that a diode is modeled as follows:

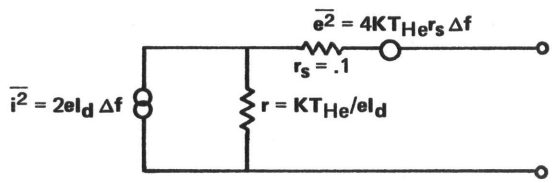

Fig. 4.1.3 – Ideal diode noise source

If such a diode were connected directly to the 50Ω input of an amplifier, and assuming that a microwatt of power were required to drive the radiometer, a quick calculation,

taking in to account the mismatch, shows that the amplifier would need gain in the order of 80 db to see the thermal noise and 100 db to see the shot noise. Since it is hoped that the shot noise will be comparable with the thermal noise, a matched gain of 90 to 100 db is required.

The amplifier chosen for this investigation was the LEL/Varian model IF30-30-02-50. The selection was based on its high gain (~90 db), its center frequency above the 1/f noise region (30 MHz), its low noise figure (~3), its 50Ω input which would be compatable with 50Ω coax, its 30 MHz or video outputs, its insusceptibility to feedback, which plagued some initial system attempts, and its narrow bandwidth (3 MHz), which would be compatable with impedance transformation techniques at 30 MHz. A number of these constraints will be discussed in succeeding sections but are best mentioned here.

The subtraction technique used in this investigation for reducing the noise figure problem also found application in establishing a frame of reference for the data. Instead of shorting the input of the amplifier during alternate samples, a variable output noise standard was connected to amplifier. Thus, for any particular laser diode fluctuation output, the noise standard was adjusted to cause the chopped signals, shown in Fig. 4.1.4, to be equal or, in other words, cause the subtractor output to go to zero. The noise standard output was then, after correcting for mismatches, identical to the noise output of the laser diode. The standard used was an AIL Hot Cold Body Standard Noise Generator in conjunction with a variable 50Ω attenuator, as shown in Fig. 4.1.5. The standard

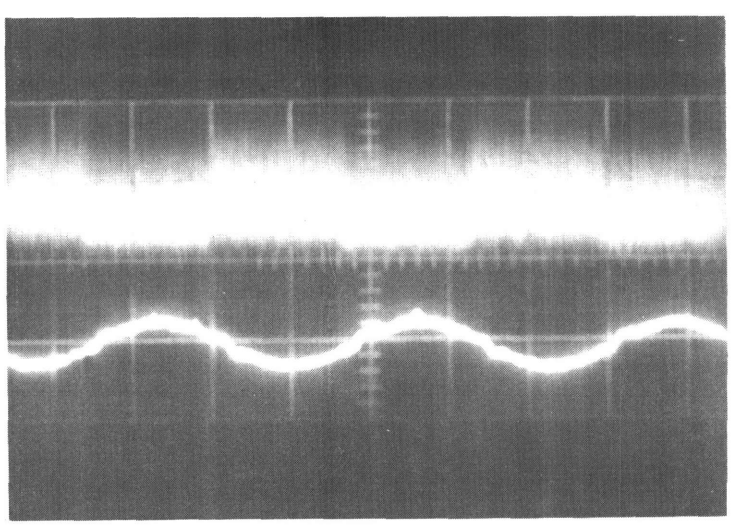

(Above) Chopped video output
(Below) Subracted output meter current

Fig. 4.1.4 – Amplifier video and subtractor outputs

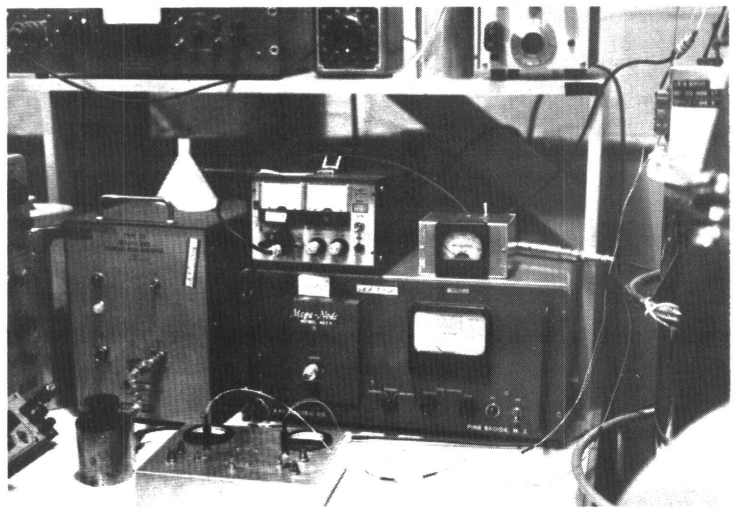

(Left) Thermal noise source and attenuator
(Below center) Shot noise source
(Center) Diode DC supply
(Right center) Diode current meter 0–800 ma and injection system
(Below) Coldfinger temperature bridges

Fig. 4.1.5 – System equipment photograph

noise generator has a constant output impedance of 50Ω and has a noise temperature of $77.3\ ^{+3^\circ}_{-0^\circ}$K maintained by liquid nitrogen. The adjustable noise output of the reference source was possible owing to the difference in temperature between an attenuator and the standard noise generator. If T_1 is the temperature of a noise source and T_2 is the temperature of a noisy network which operates on the noise fluctuations from T_1, then the noise power delivered to a matched load is given by

$$P = G_2 kT_1\ \Delta f + (1 - G_2) kT_2\ \Delta f \tag{4.1.1}$$

where G_2 is the gain of the network. In this case $T_1 = 77.3^\circ$K, $T_2 = 290^\circ$K, and G_2 is the gain of the attenuator. Thus, the reference available noise power can be adjusted between $kT_1\ \Delta f$ and $kT_2\ \Delta f$. For larger noise powers a Kay Electric standard shot noise generator, shown in Fig. 4.1.5, with diode currents up to 100 ma was available.

4.2 Dewar assembly

In the previous section, methods of handling the laser diode noise were discussed. The emphasis in this section will shift to the acquisition of the noise from the diode itself. A very important part of this process was selection of the diodes to be used. It was decided that there were enough variables in the experiment already, and to use

pulsed laser excitation was to unjustifiably add to the confusion. Thus, it was necessary to select diodes which would lase under continuous excitation. Lasers fabricated at the University of Wisconsin were found to be of higher quality than those of some commercial sources in this respect.[18] The selection techniques used in evaluating these diodes are discussed in Appendix A.

Continuous excitation imposed its own set of constraints on the investigation. The most obvious of these is the need to cool the diodes to a temperature such that the threshold condition is continuously maintained at some convenient current level. Proebsting found that above 50°K threshold increased as $T^{5/2}$ and, for lower temperatures, increased exponentially with T.[18] Calculations from that investigation showed that in order to obtain the threshold condition below 500 ma for laser H-52 it was necessary to keep its temperature below 40°K. Liquid helium was therefore employed as the cooling agent. The helium was contained by a cylindrical glass dewar of 50″ in length, which was in turn bathed in liquid nitrogen contained in a metal dewar, shown in Fig. 4.1.2. The geometry of the dewar required airtight construction and evacuation procedures to prevent water vapor from accumulating and freezing within the dewar.

In order to retain the option of holding the laser above as well as below the liquid level while maintaining its low temperatures, in the case that extreme perturbations of the light output should be effected by the liquid, a coldfinger heat sinking arrangement, shown in Fig. 4.2.1a,b, was used. Other constraints of equal importance were the routing of wires through the liquid helium before termination at the laser in order to reduce thermal conduction from without the dewar; the operation of the laser as close to the bottom of the 50″ dewar as possible in order to improve the placement of the laser relative to the thermal gradient between the liquid and the mouth of the dewar; the use of thin wires to increase the thermal resistance; and the use of bakelite tubing for coldfinger support and wire conduit to prevent high vaporization rates of the liquid helium.

Optical and electrical constraints on the dewar system were no less demanding. Several methods described by Proebsting and Magee for determining laser threshold attainment were applied in this investigation. They consist of detecting the light emitted by the diode after being passed through a polarizer. Not only does the light intensity increase markedly but polarization perpendicular to the junction plane results at threshold. Thus, in order to make use of these techniques it was necessary to orient the laser on the coldfinger such that its light would pass up the dewar through a polarizer and to a photomultiplier tube. The dewar assembly on which the polarizer and photomultiplier were mounted also passed the wires and support tube for the coldfinger assembly. As

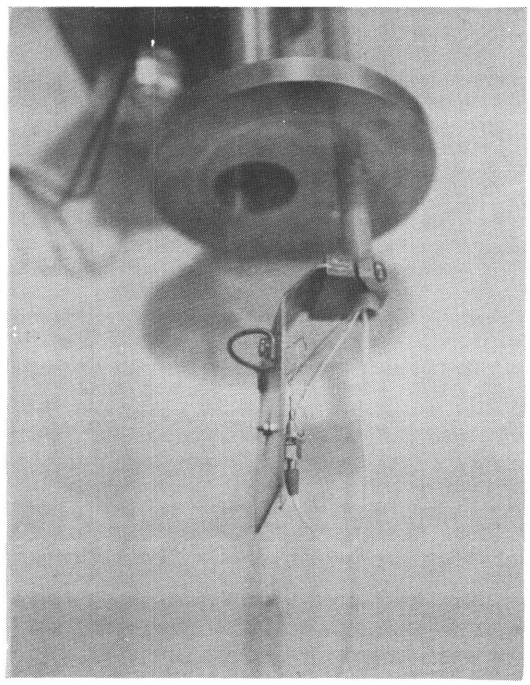

Laser on TO header is screwed to copper heat sink

(a)

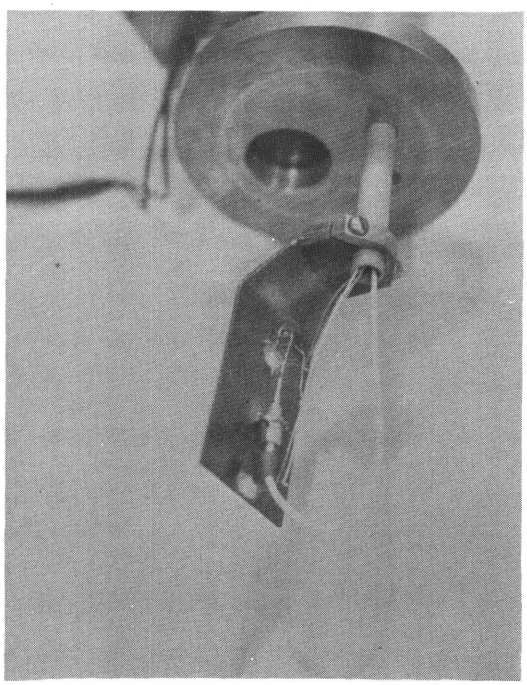

Vacuum sealed optical window

50Ω microdot coax dips into He before reaching heat sink and laser

Thermal sensing resistors mounted with epoxy

(b)

Fig. 4.2.1 – Coldfinger assembly

will be evident later, it was very necessary for the characteristic impedance of the cable to the laser to be unperturbed by feed through insulators. Therefore, at the point where the wires left the bakelite tubing above the dewar, an epoxy seal was made.

The dewar assembly, Fig. 4.2.2, consisted of a flat plate having an O-ring bottom surface to fit the dewar with a vacuum seal and having both optical and electrical outlet holes as well as a helium transfer tube inlet hole. The electrical output hole was fitted with a vacuum quick couple, through which the bakelite tube was passed to enable the raising and lowering of the coldfinger. The optical hole was fitted with an airtight window which lay between the bottom plate and an upper light-tight cylinder. The cylinder housed a polarizer assembly which was rotated at 10 rpm by a small motor. An Electro Optics Associates cooled photomultiplier assembly, PM101, using a 7102 photomultiplier tube was screwed into the top of the light-tight cylinder. As the polarizer rotated, a diode above threshold could be readily distinguished by the large periodically varying voltage excursions displayed on a Keithley 151 microvoltmeter.

The coldfinger assembly, shown in Fig. 4.2.1, was made of copper to provide good thermal conduction from the diode's header to the helium bath. Located at the bottom of

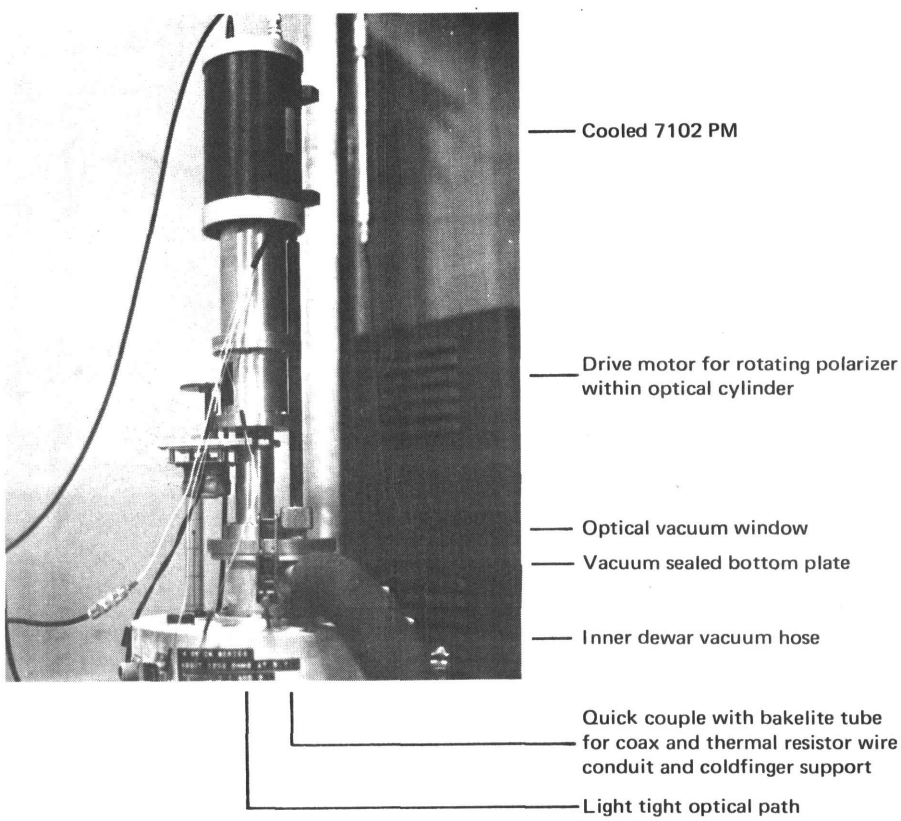

Fig. 4.2.2 – Dewar assembly

the sink and again just below the laser level, were two 1/4 watt 130Ω resistors used as liquid helium level indicators. They were connected to the bridge circuits shown in Fig. 4.1.5 and 4.2.3. As the temperature changed, the bridge was unbalanced to varying degrees. A distinct change in the balance resulted as the resistors passed the liquid level itself.

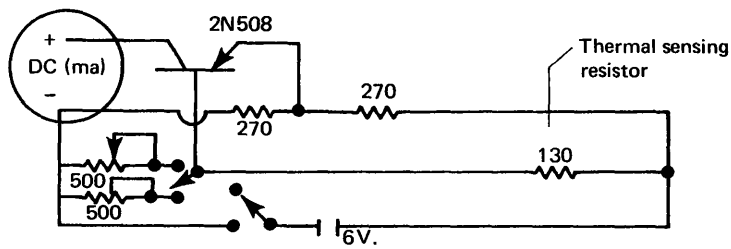

Fig. 4.2.3 – Liquid helium level indicator

4.3 Noise transmission

With both noise generation and measurement techniques having been discussed, there remains only the need to analyze the noise transmission between the laser diode and the measurement apparatus. The three basic concepts which must be integrated and applied to solve this problem are impedance matching for maximum power transfer, impedance transformation effects at 30 MHz, and system losses. The problem, though theoretically a simple task, is complicated by the extremely low impedance of the diode.

The fundamental difficulty to be alleviated is the absense of any knowledge about the proportion of diode noise which is transferred to the amplifier. Consider the diagram in Fig. 4.3.1. It is evident that the subtraction technique used in this investigation

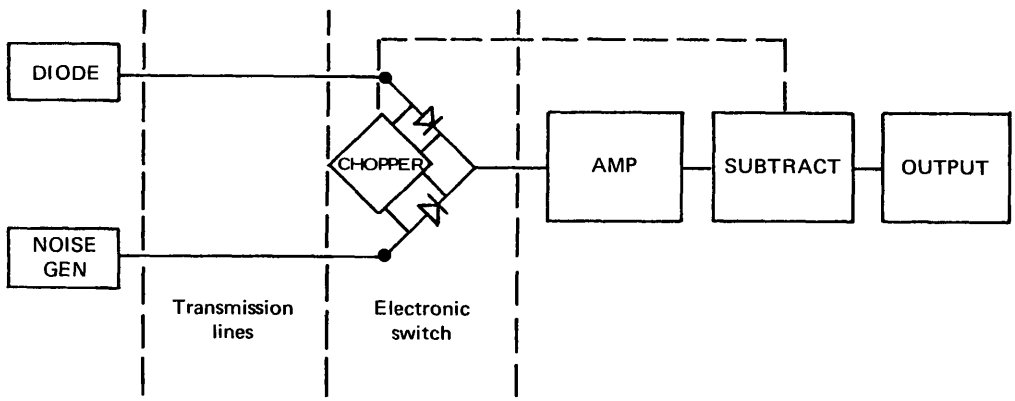

Fig. 4.3.1 – Noise transmission system schematic

could, in addition to "eliminating" amplifier noise, subtract out transmission effects. However, this would demand that the standard noise generator have an output impedance identical to that of the diode and that the transmission systems of the diode and noise generator be identical, both extremely difficult requirements to meet. A more reasonable approach and one which is probably every bit as accurate as any other method, is the calculation of mismatches and losses from sound electrical principles.

To use this approach it is first necessary to calculate the fraction of the diode current fluctuation which reaches the amplifier. Consider a transmission line having a characteristic impedance, $Z_0 = 50\Omega$, which connects an ideal laser diode to a load Z_L as shown in Fig. 4.3.2.

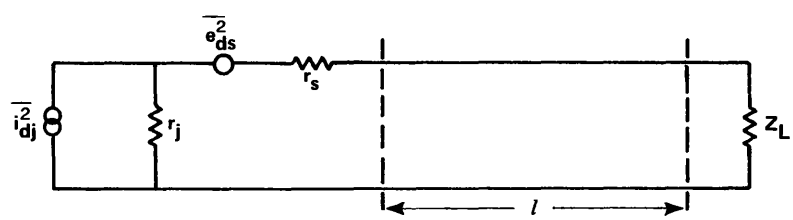

Fig. 4.3.2 – Ideal noise transmission schematic

This is more generally depicted in Fig. 4.3.3 as

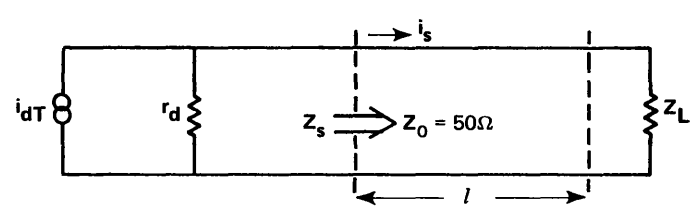

Fig. 4.3.3 – Current equivalent noise transmission schematic

From elementary transmission line theory

$$\rho_L = \frac{Z_L - Z_0}{Z_L + Z_0} \tag{4.3.1}$$

$$Z_s = Z_0 \frac{1 + \rho_L e^{-2j\beta l}}{1 - \rho_L e^{-2j\beta l}} \tag{4.3.2}$$

$$i_s = i_{dT} \frac{r_d}{r_d + Z_s} \tag{4.3.3}$$

$$i_s = i_L \frac{(1 - \rho_L e^{-2j\beta l})}{(1 - \rho_L) e^{-j\beta l}} \tag{4.3.4}$$

Equating 4.3.3 and 4.3.4, and substituting for Z_s and then for ρ_L,

$$i_L = i_{dT} \frac{2r_d Z_0}{(Z_0 + Z_L)(Z_0 + r_d) e^{+j\beta l} + (Z_0 - Z_L)(r_d - Z_0) e^{-j\beta l}} \tag{4.3.5}$$

Now Z_L is seen in Fig. 4.3.1 to be the impedance looking into the electronic switch or chopper. It is evident from the above expression that the fraction of the current through Z_L will be independent of the line length if $Z_L = Z_0$. In pursuit of this simplification the input impedance of the amplifier was measured with an RX-25A impedance bridge, using reduced power so as not to saturate the amplifier. It measured 43Ω. The switch was connected to this input by 6″ of 50Ω coax. The input impedance of the switch measured 46Ω. Referring again to the equation for i_L, and remembering that r_d is on the order of .1Ω, note that

$$(Z_0 + Z_L)(Z_0 + r_d) \approx 4{,}800$$

while

$$(Z_0 - Z_L)(r_d - Z_0) \approx 200$$

But even though the magnitude of the vector addition in the denominator of 4.3.5 will vary as much as 400 out of 4800Ω as the line length is varied, the approximation will be made that $(Z_0 + Z_L)(Z_0 + r_d)$ is the only term of significance, i.e., that the load is matched to the line, such that

$$i_L = i_{dT} \frac{2r_d Z_0}{(Z_0 + Z_L)(Z_0 + r_d)} = i_{dT} \frac{r_d}{Z_0 + r_d} \tag{4.3.6}$$

It should be obvious that the above development also applies to the transmission of noise fluctuations from the reference noise source if r_d is replaced by r_r, and i_{dT} by i_r. Since $r_r = 50\Omega$, the relation

$$i_L = i_r \frac{2r_r Z_0}{(Z_0 + Z_L) 2Z_0} = i_r \frac{r_r}{Z_0 + Z_L} \tag{4.3.7}$$

is exact, no matter what length of line is used. And if it is again assumed that the load is matched to the line,

$$i_L = i_r. \tag{4.3.8}$$

It would appear from 4.3.6 and 4.3.8 that if one disregards the mismatch at the load and any asymmetry in the electronic switch, we would have that

$$i_{dT} \frac{r_d}{Z_0 + r_d} = i_r. \tag{4.3.9}$$

But until now the transmission lines have been assumed to be lossless. Since such is not the case, both the attenuation of the noise from the source and the addition of noise power at 290°K by the lines must enter the above calculations. This procedure is similar to the one used when combining the reference noise source at 77°K and the attenuator at 290°K. The line loss is given by e^{-al}, so that if P_{in} and P_{out} represent the powers into and out of the line loss, then

$$P_{out} = P_{in}\, e^{-al} + (1 - e^{-al}) KT_{290}\, \Delta f \tag{4.3.10}$$

Finally, if the output of the subtractor is made to null by varying the output of the reference noise source in order to take a data point

$$P_{Ld\,out} = P_{Lr\,out} \tag{4.3.11}$$

Substituting 4.3.10 for the diode and reference sides into 4.3.11, we have,

$$P_{Ld\,in}\, e^{-al_d} + (1 - e^{-al_d}) KT_{290}\, \Delta f = P_{Lr\,in}\, e^{-al_r} + (1 - e^{-al_r}) KT_{290}\, \Delta f \tag{4.3.12}$$

Now, with application of 4.3.6,

$$P_{Ld\,in} = \overline{i_{dT}^2} \left(\frac{r_d}{Z_0 + r_d} \right)^2 Z_L \tag{4.3.13}$$

and using 4.1.1,

$$P_{Lr\,in} = KT_{77}\, \Delta f\, G + (1 - G) KT_{290}\, \Delta f \tag{4.3.14}$$

such that 4.3.12, 4.3.13 and 4.3.14 are combined to give

$$\overline{i_{dT}^2}\left(\frac{r_d}{Z_0 + r_d}\right)^2 Z_L\, e^{-al_d} + (1 - e^{-al_d})\,KT_{290}\,\Delta f$$

$$= \Delta f\,(KT_{77}\,G + (1 - G)\,KT_{290})\,e^{-al_r} + (1 - e^{-al_r})\,KT_{290}\,\Delta f \quad (4.3.15)$$

Letting $G \equiv 10^{-C_a}$, $e^{-al_d} \equiv 10^{-C_d}$, and $e^{-al_r} \equiv 10^{-C_r}$ the previous equation becomes

$$\frac{\overline{i_{dT}^2}}{\Delta f}\left\{\frac{r_d}{Z_0 + r_d}\right\}^2 Z_L\, 10^{-C_d} + \left\{1 - 10^{-C_d}\right\}KT_{290}$$

$$= \left\{KT_{77}\,10^{-C_a} + (1 - 10^{-C_a})\,KT_{290}\right\}10^{-C_r} + \left\{1 - 10^{-C_r}\right\}KT_{290} \quad (4.3.16)$$

This expression may be simplified since

$$r_d \ll Z_0, \qquad Z_L \approx Z_0$$

such that

$$\frac{\overline{i_{dT}^2}}{\Delta f} = \frac{Z_0 K}{r_d^2}\left\{T_{290} - (T_{290} - T_{77})\,10^{C_d - C_r}\,10^{-C_a}\right\} \quad (4.3.17)$$

The above equation will be used in the next chapter for analysis of the data obtained in this investigation. But it is of interest at this point to discuss further the implication of losses in the transmission system and methods of dealing with them.

4.4 Impedance transformation

It was necessary, in section 4.3, to include line loss effects in the expression relating the diode noise power to that of the reference noise source. However, the problem is more severe than a mere requirement of compensation during calculations. In fact, line loss can wash out the noise from the diode just as amplifier noise can, due to the imprecision of the subtraction electronics, although here we are more concerned with the imprecision of line loss measuring techniques.

The severity of the line loss problem results directly from the mismatch between the diode and the transmission system. Although line loss is quite small, the fact that the power entering this line from the diode is already reduced by $(r_d/Z_0 + r_d)^2$ and that the losses in the line are at 290°K made the problem sufficiently important to be treated in this investigation. Since there is little that can be done about the lines' temperature, the

feasibility of making a matching device was investigated. Initial attempts at matching involved the use of ferrite and air core transformers. It was found that both the wide divergence of the impedances to be matched, ~0.1 to 50 ohms, and the fact that the diode impedance was small made it impossible to obtain good coupling of power. Special methods were necessary if straight transformers were to be useful.[19] Still another attempt involved the use of tuned coupled circuits.[20] Although it was again possible to match impedances that were not widely divergent with almost no loss, for the impedances of interest here, it was not possible to get reasonable matching unless each side was tuned to the same frequency and coupling was low. In otherwords it was necessary to go to bandwidths as narrow as ~0.2 MHz. As the amplifier had a bandwidth of 3 MHz it would have been necessary to either account for the bandwidth differences in the calculations for $\overline{i_{dT}^{L}}$, or to make a filter for the reference source having the identical frequency response as that for the diode. Neither of the methods were considered accurate enough to be worthwhile, especially since the match was still not good. Stub tuning which is discussed in Appendix B was found to have losses of ~7 dbm with bandwidths not much better than 3 MHz. As a result, it was decided that common techniques of impedance matching were not applicable to the impedances, frequencies, and low loss requirements of this investigation. That such techniques have been used in other noise investigations is attributable to the fact that these investigations have all been at low current levels and high enough temperature where impedances of the diodes are at least 5Ω. The data in the following chapter was taken, therefore, without the benefit of impedance transformation.

CHAPTER 5

Data Analysis

Measurements were made on three different diodes. A total of five runs were made on the diodes, including one under liquid nitrogen. Of the three diodes, only one lased and it did so under liquid He. In the first section the curves of $\overline{i_{dT}^2}$ as a function of the injection current will be given, the data itself being given in Appendix C. The implications of these results will be discussed in the context of the preceding three chapters in section 5.2.

5.1 Presentation of results

In section 4.3 an expression was developed to relate the reference source attenuation in the measurement system to the noise current from the laser diode. This relation

$$\frac{\overline{i_{dT}^2}}{\Delta f} = \frac{Z_0 k}{r_d^2}\left\{T_{290} - (T_{290} - T_{77})\, 10^{C_d - C_r}\, 10^{-C_a}\right\} \tag{5.1.1}$$

will for the moment be accepted as correct. If it is to be used, the resistance of the diode and attenuations due to line loss must be determined. In chapter 2 it was shown that a low current model for a diode is represented by a shot noise current source in parallel with the junction, all in series with a thermal noise voltage source and the bulk resistance as in Fig. 5.1.1a. From Thevenin's theorem we later used the model shown in Fig. 5.1.1b. In order to determine the size of r_d, the impedance as a function of injection

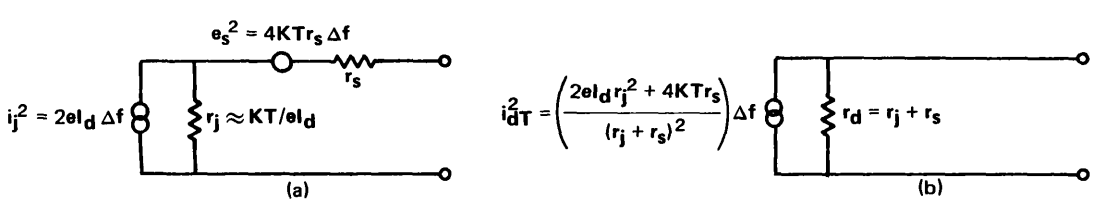

Fig. 5.1.1 – Ideal low current diode noise equivalent circuits

current was viewed at 1/4 wavelength away from the diode H-31 in liquid nitrogen. The results are listed in Table I. The diode end of the line was then shorted, and the impedance was measured as 580Ω. If the values in Table I are transformed around the Smith chart, the impedances obtained would not be the diode impedance, again due to line loss. The fact that a short transforms to 580Ω makes the point clear. But since we have measured $Z^{l}_{1/4\lambda} = 580\Omega$ as well as $Z^{t}_{1/4\lambda}$ and since Z_0, the characteristic impedance is known, we can transform back to the diode impedance. We know that

$$A_{dl} \equiv e^{-2\alpha l_{1/4\lambda}} = \left|\rho^{l}_{1/4\lambda}\right| \tag{5.1.2}$$

Also by definition

$$\left|\frac{Z^{t}_{1/4\lambda} - Z_0}{Z^{t}_{1/4\lambda} + Z_0}\right| \equiv \left|\rho^{t}_{1/4\lambda}\right| \tag{5.1.3}$$

$$\left|\frac{Z^{l}_{1/4\lambda} - Z_0}{Z^{l}_{1/4\lambda} + Z_0}\right| \equiv \left|\rho^{l}_{1/4\lambda}\right| \tag{5.1.4}$$

$$\left|\frac{r_d - Z_0}{r_d + Z_0}\right| \equiv \left|\rho^{d}_{0\lambda}\right| \tag{5.1.5}$$

Since

$$\left|\rho^{d}_{0\lambda}\right| A_{dl} = \left|\rho^{t}_{1/4\lambda}\right| \tag{5.1.6}$$

we have

$$\left|\frac{r_d - Z_0}{r_d + Z_0}\right| = \frac{\left|\dfrac{Z^{t}_{1/4\lambda} - Z_0}{Z^{t}_{1/4\lambda} + Z_0}\right|}{\left|\dfrac{Z^{l}_{1/4\lambda} - Z_0}{Z^{l}_{1/4\lambda} + Z_0}\right|} \tag{5.1.7}$$

It is then possible to solve for r_d and arrive at Table II. These results appear to be reasonable. As the current increases, the diode resistance decreases just as it should according to $r_j = KT/eI_d$ until at high currents r_j becomes small enough that r_s, the bulk resistance, takes over. Bulk dc resistances were measured for these diodes by Proebsting.[18] The value for H-31 was 0.07 ohms and that for H-52, another diode used in this investigation, was 0.20 ohms. It is difficult to choose a precise value for r_d. For

Table I

I_d(ma)	$\left\lvert Z^T_{1/4\lambda}\right\rvert$(ohms)
145	536.0
245	541.5
315	543.5
355	544.5
395	545.0
710	546.0

Table II

I_d(ma)	r_d	$(r_d/r_s)^2$
145	0.357	1.70
245	0.309	1.30
315	0.292	1.13
355	0.287	1.12
395	0.282	1.08
710	0.272	1.00

our purposes, we let $r_d = 0.1$ ohm, acknowledging that the magnitude of the results will be off by a small factor, and then take into account the change in r_d with I_d by insertion of of $(r_d/r_s)^2$ from Table II into the formula for $\overline{i^2_{dT}}$.

Before using equation 5.1.1, it is still necessary to determine C_d and C_r. Using a sweep generator in conjunction with a variable attenuator it was determined that the reference line had an attenuation of ~0.35 dbm and that the line from the diode had an attenuation of ~0.9 dbm.

The relation for calculation of the total noise current from a laser diode is now given as

$$\frac{\overline{i^2_{dT}}}{\Delta f} = \frac{50 \times 1.38 \times 10^{-23}}{(r_d/r_s)^2(.1)^2}\left\{290 - 242 \times 10^{-C_a}\right\} \tag{5.1.8}$$

Using the data in Appendix C for C_a and the measured values for $(r_d/r_s)^2$ contained in Table II, the curves shown in Fig. 5.1.2 and Fig. 5.1.3 can now be calculated. In Fig. 5.1.2, both the curves resulting from $(r_d/r_s)^2 = 1$ and those resulting from $(r_d/r_s)^2$ which assumes the values of Table II are presented. Fig. 5.1.3, however, shows only those curves derived using Table II, since the junction resistance, r_j, does indeed become comparable with r_s for the lower injection currents as was alluded to at the end of section 3.2. The data in Fig. 5.1.3 is plotted along with curves obtained by Strutt, which have already been discussed in chapter 3, as well as with the curve which would result if $\overline{i^2_{dT}}$ were a pure $\overline{i^2}/\Delta f = 2eI$ shot noise generator.

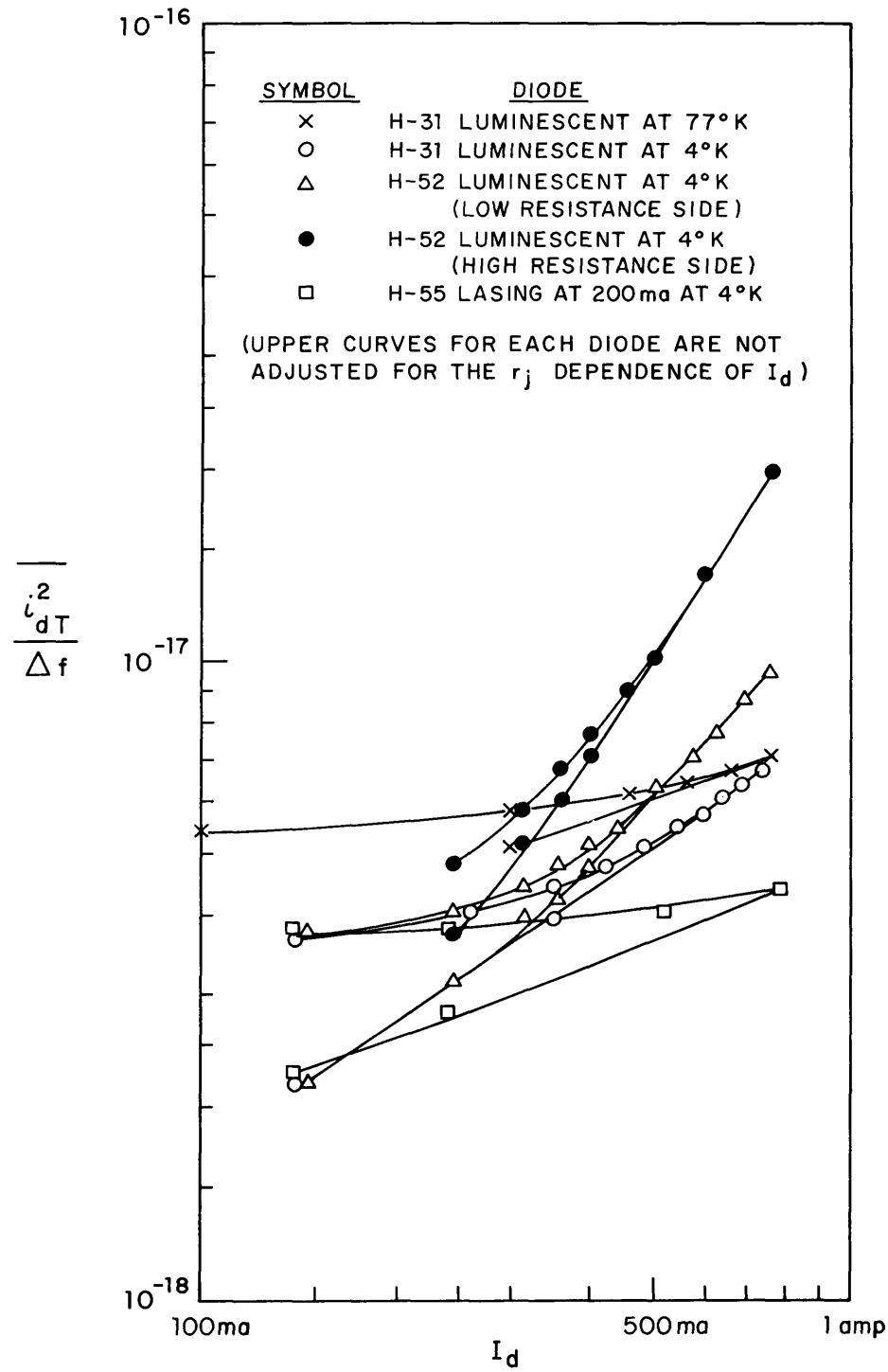

Fig. 5.1.2 – Measured noise current as a function of injection current

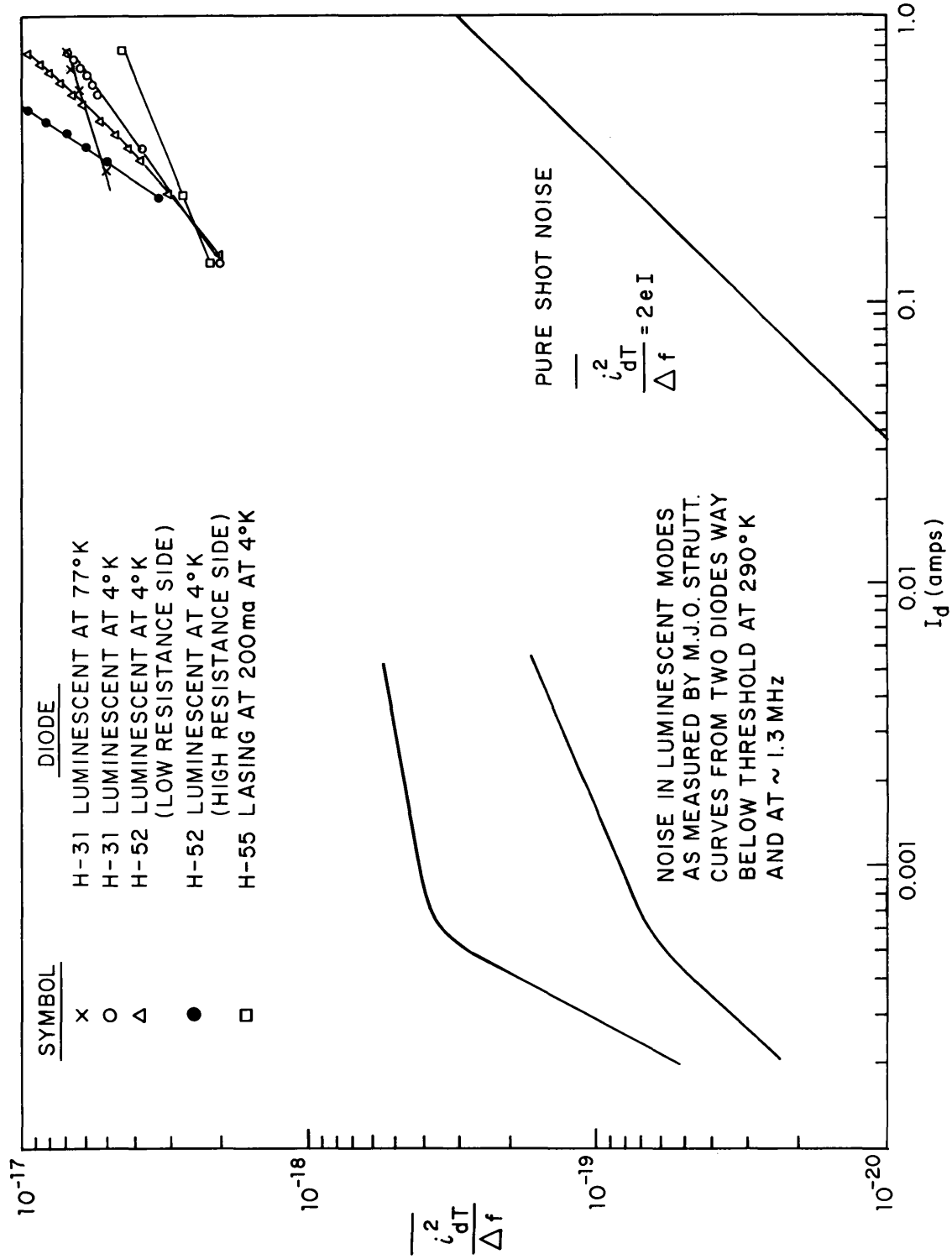

Fig. 5.1.3 – Related noise current data as a function of injection current

5.2 Interpretation of results

It was apparent from chapters 2 and 3 that one should refrain from trying to formulate precise relationships for the noise in laser diodes, at high injection currents, on the basis of presently existing theories. Thus, the problem was approached from the viewpoint of obtaining data that described the total noise current output and then noting any resulting similarities to existing noise theories. Considering the curves of Fig. 5.1.3, it would be difficult to say much about the relationship of $\overline{i_{dT}^2}$ to I_d from an independent analysis of each curve. It is interesting however to observe that the curve for H-31 at 4°K is below that for H-31 at 77°K. Also, one would expect that a diode with narrower cross section than but an identical current to another diode would heat up to a greater degree than that second diode. Indeed it is seen that the narrow side of H-52 has a higher curve than the wide side. Suspicions are given credence when the only diode to lase, H-55, is shown in Fig. 5.1.3 to have a curve below those of the other diodes. Although it can not be firmly established that the predominant noise is thermal in origin, it is at least a good possibility.

In addition to the apparent wash out of other effects by the diodes' own thermal noise, the existence of relatively few data points for H-55 is evidence of a second and equally as deleterious thermal effect. This problem, discussed in sections 4.3 and 4.4, is caused by the necessarily long transmission lines for this particular liquid helium set up, and the resulting line loss and line noise temperatures. The point is reached where a change in noise from the diode is so small compared to the existing noise temperature of the lines, that subtraction is not precise enough to accurately yield that change in the diode noise. Essentially a subtraction of 1 – 1 is approached, and only two or three data points can result even if the injection current is pushed to 800 ma.

CHAPTER 6

Conclusions

Although the results given in chapter 5 were not particularly positive in the sense of unequivocal support of a particular noise theory, they were the best results obtainable with conventional measurement techniques. There were a number of conflicting constraints imposed upon this investigation. In 2.1 it was seen that the equivalent shot noise resistance of a diode according to one theory was almost identical with the diode's thermal noise resistance at room temperature and became less than the thermal noise resistance by nearly 2 orders of magnitude as the temperature decreased to helium temperatures. It was found necessary in 4.2, on the other hand, to operate the diodes at liquid He temperatures in order to achieve lasing action. Immediately, it appeared that we were restricted either to low current luminescent modes and the chance of some uninteresting shot effect mixed with thermal noise or to high current lasing with not much chance of seeing anything but thermal noise. However, discussions of high current operation in 2.2 and 2.3 indicated that more shot noise should result for high injections than was calculated by low current theories. The decision to attempt measurements at high injection currents was firmly made after measurements by Strutt, reported in 3.2, showed shot noise at low injection currents in GaAs laser diodes to be more than two orders of magnitude higher than the existing low current theories predicted. As has been seen from 5.2, however, no clear cut definition of the noise type present in a high injection lasing diode resulted from the measurements of this investigation. It was postulated that the noise was predominantly thermal in origin. Whether or not another improved experimental system would yield more well-defined results is open to question. Certainly these measurements were made at frequencies 30 times those of Strutt, and it is true that state-of-the-art transformers exist for transformation between the impedances encountered in this investigation. However, new diodes would have to be fabricated and adapted to these techniques, which are presently withheld from public dissemination. Furthermore, it is believed significant that the investigation by Strutt, although a response to Haug's theoretical work, did not even come near to dealing with currents around threshold, the

region of primary concern in Haug's work. And there is no good reason to believe that the results at 1–5 MHz should be much different from those at 30 MHz.

In this investigation several fairly unique techniques have been adopted. It seems that the chop and subtract technique for reduction of background noise problems, while finding application in the noise analysis of conglomerate electronic devices, such as receiver front ends, has heretofore not been used in experiments on individual electronic components, such as transistors and diodes. It is felt that this technique represents a significant improvement in the reliability of the measurement system. Also of considerable importance was the entry of line loss and its associated thermal noise into the calculations of this investigation.

If further attempts are to be made to search for the shot effects near threshold, the noise phenomenon described in chapter 1 as being of singular interest in a laser diode, all evidence from this investigation points to a need for several major changes in the experimental setup. In the latter part of section 3.2 and later in section 5.1, the chance that the shot noise might be less than the thermal fluctuations, due to the necessity of operating at 4°K and the requirement of high threshold currents, was acknowledged. The experimental results seem to substantiate that this is indeed the case, and Van der Ziel is in agreement with these results.[21] In order to reduce such thermal effects it would be desirable to fabricate diodes which would lase at higher temperatures and lower injection currents. Then because $r_j \approx KT/eI$ would be larger, the chances of seeing the shot noise across the junction would be improved. Such a change would induce other revisions which themselves would have beneficial effects. Operation at 77°K, for example, would allow a smaller dewar to be used, which would in turn allow shorter transmission line lengths and thus lower line losses and line temperature effects. Such diodes could also be fabricated in consort with state-of-the-art transformer fabrication mentioned earlier in this chapter in order that the mismatch might be alleviated. It is, finally, also recommended that lower frequencies be used with such a transformer in order that high frequency spurious and transmission line effects will no longer be a problem.

ADDENDUM

Following the writing of this report, a paper by Guekos and Strutt[22] appeared and still another was referenced[23] which were concerned with the measurement of noise in GaAs diode lasers in the region of threshold. The reported measurements were made with a diode temperature of 77°K and at a frequency of 58 kHz. The data values were not absolute, but instead were referenced to that noise output of the diode at 400 ma, threshold in the neighborhood of 600-800 ma.

The reported curves of normalized noise voltage as a function of injection current show that a relative maximum of about 2 times the 400 ma value occurs at threshold (600 ma). Several successive relative maxima appear up through injection currents of 900 ma, with noise increases of as much as three and four orders of magnitude over the 600 ma value. These results correlated in all but one of the maxima with curves taken of the light field fluctuations for the same diode. That the maxima also correlated with the appearance of lasing filaments in the junction adds still more credence to the results.

It is interesting to note that the changes in the experimental setup recommended in chapter 6 of this report are incorporated in the system used by Strutt. Not only were good-quality lasers obtained from IBM, such that cw operation at 77°K was possible, but a low frequency amplification system and a "matching" transformer were used.

Strutt's apparent success in obtaining good results seems to attest to the validity of the recommendations in chapter 6. It appears reasonable that implementation of these changes would have allowed the effects observed by Strutt to appear above the thermal noise found in our measurements.

Still open to question, however, is the effect of frequency upon the measurements. Strutt's reported values are at 58 kHz, while the measurements in this report were taken at 30 MHz. Strutt did take some unreported data at 6 MHz and stated that the results were qualitatively similar to those at 58 kHz. But it is interesting that the reported data is in the 1/f region.

APPENDIX A

If laser diodes were to be found which would operate continuously at liquid helium temperatures, it was necessary to select them from a batch of 32 diodes. In order that the diodes would not be significantly effected by heating during the selection process, pulsed operation at 77°K was employed. It was believed that the best pulsed lasers would give an indication of the probability of continuous operation at 4°K.

The experimental setup is shown in Fig. A.1. The assembly consisted of a nitrogen dewar with a coldfinger for laser mounting and a prism at the top of the dewar for light monitoring. The light passed through a rotating polarizer and a 0.84μ filter before being detected by a cooled 7102 photomultiplier tube. The photomultiplier output, working into 50 ohms, was amplified and displayed on a Textronix 503 oscilloscope. A current sample from the pulser was displayed on another 503 scope. Both scopes were triggered by the pulser. The pulser was of low output impedance and supplied as much as 10 amps. Pulse width and amplitude as well as the repetition rate were variable.

The results of short pulse (2 μsec) operation on diode H-26 cooled with liquid nitrogen are shown in Fig. A.2a,b for luminescent output and in Fig. A.3a,b for the lasing output. As pulse widths were increased to 200 μsec significant Joule heating effect was observed as one progressed through the width of the pulse even though T = 4°K. Figure A.4a,b shows luminescent operation of H-26, and Fig. A.5a,b shows its lasing output. Table A-I is a listing of all but two of the diodes tested. A 5 μsec pulse width was maintained, and liquid nitrogen was used for cooling. The diode is rated by its threshold current and repetition rate. One side of diode H-49 had a repetition rate of $(50\ \mu\text{sec})^{-1}$ and a threshold of ~4 amps. Diode H-55 was nearly as good with $(50\ \mu\text{sec})^{-1}$ at 4.5 amps. The diodes not tested, H-31 and H-52, proved during noise measurements to be nonlasing. Since H-49 appeared to be very good, it was tested at 4°K using 7-msec pulses at $(8\ \text{msec})^{-1}$ repetition rate. Lasing over the entire pulse length did occur. Unfortunately, after several test runs under continuous operation with threshold of 500 ma the heat evidentally deteriorated the junction and H-49 ceased to lase continuously. A recheck of its 77°K 5-μsec pulsed characteristics showed that they had deteriorated to 7 amps threshold

at (80 μsec)$^{-1}$ repetition rate. With this in mind H-55 was not operated continuously until noise measurements were made, at which time it lased continuously at 200 ma and continued to do so at least up to 800 ma.

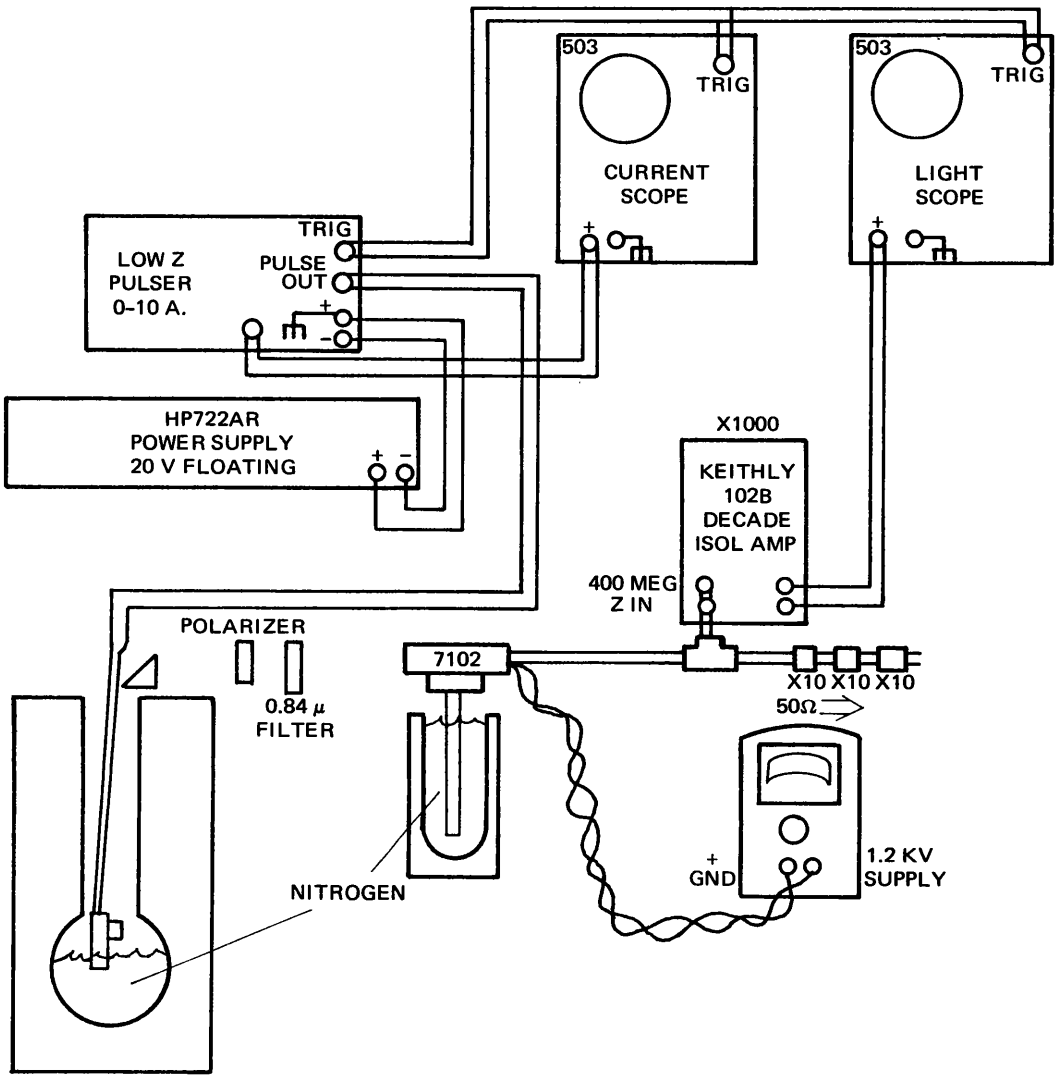

Fig. A.1 – Laser test system schematic

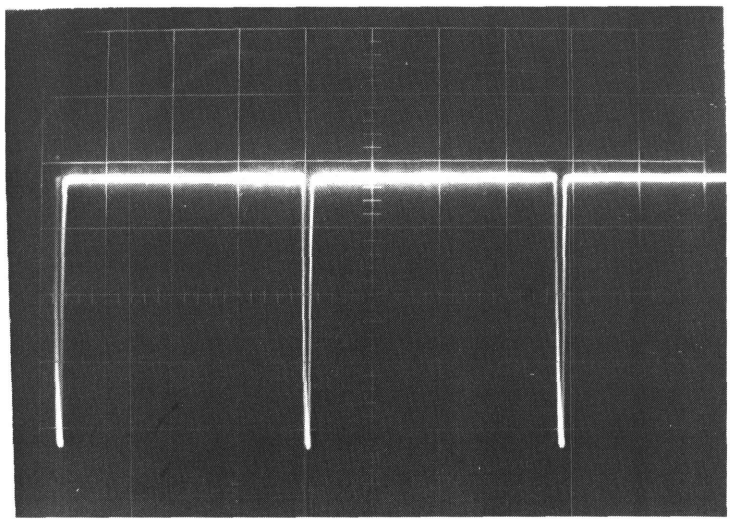

(a)
Diode H-26 current just below threshold
Current pulses are negatively directed
2 amps/cm vertical
50 μsec/cm horizontal

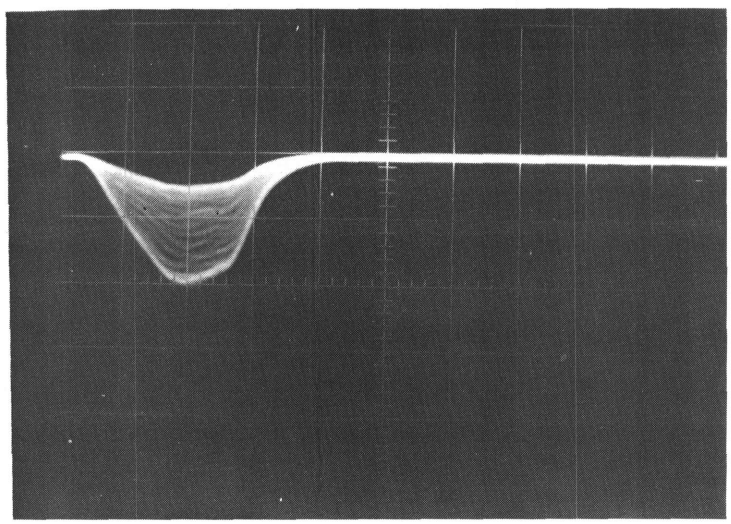

(b)
Diode H-26 light output just below threshold
Pulse is negatively directed
T = 77°K
2 μsec/cm horizontal

Fig. A.2 – Subthreshold laser short pulsed

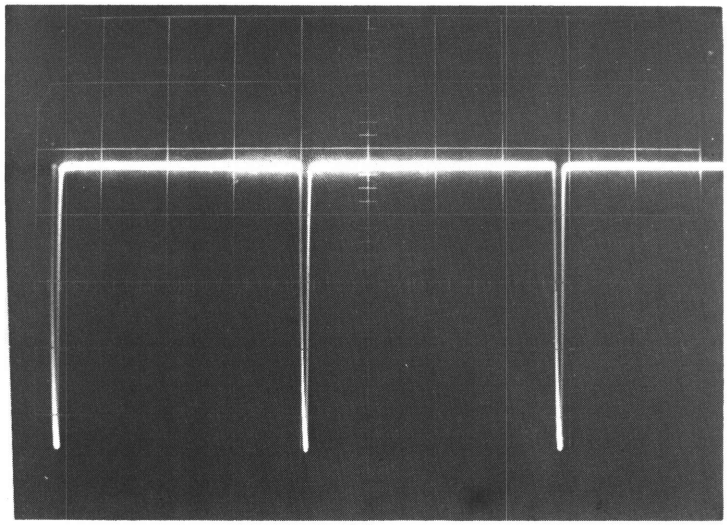

(a)
Diode H-26 current just above threshold
Current pulses are negatively directed
2 amps/cm vertical
50 μsec/cm horizontal

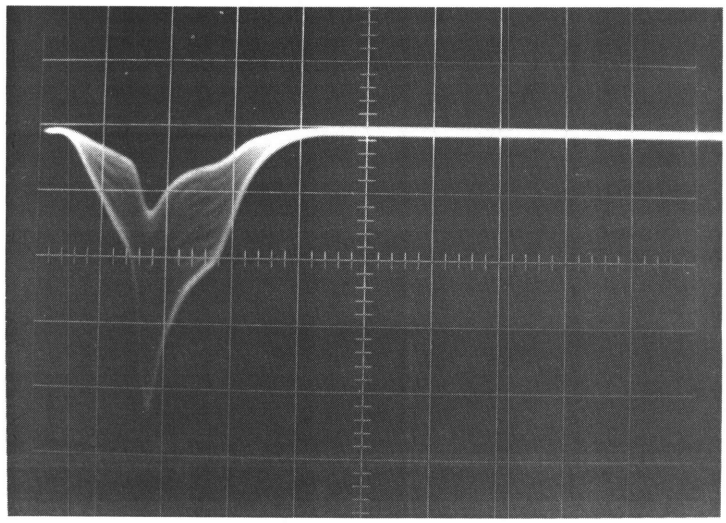

(b)
Diode H-26 light output just above threshold
Pulse is negatively directed
T = 77°K
2 μsec/cm horizontal

Fig. A.3 – Above threshold laser short pulsed

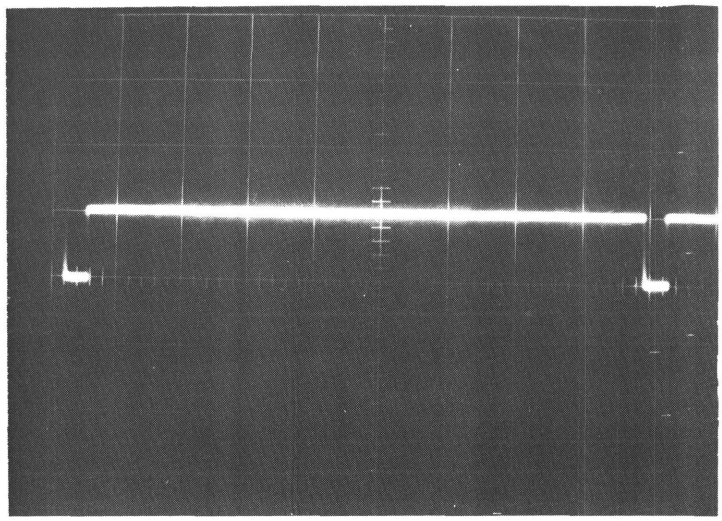

(a)
Diode H-26 current just below threshold
Current pulses are negatively directed
0.5 amps/cm vertical
0.5 msec/cm horizontal

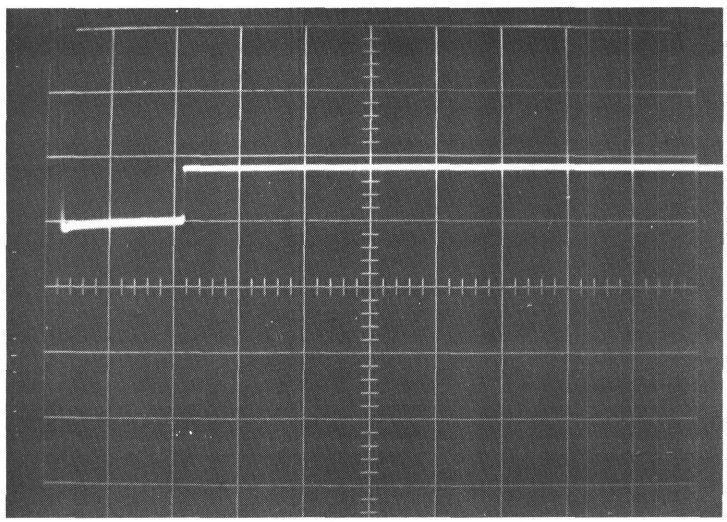

(b)
Diode H-26 light output just below threshold
Pulse is negatively directed
T = 4°K
0.1 msec/cm horizontal

Fig. A.4 – Subthreshold laser long pulsed

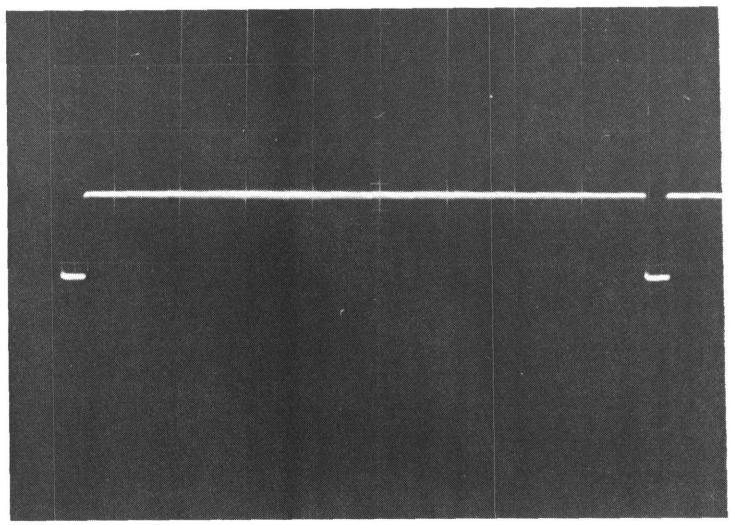

(a)
Diode H-26 current just above threshold
Current pulses are directed negatively
0.5 amps/cm vertical
0.5 msec/cm horizontal

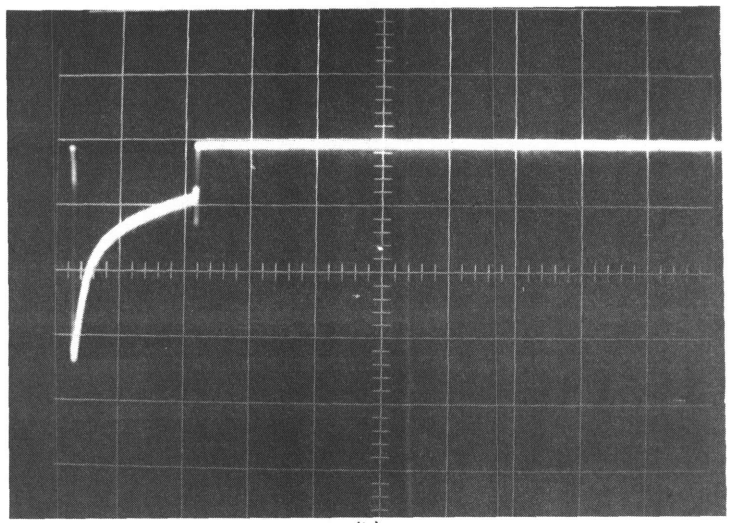

(b)
Diode H-26 light output just above threshold
Pulse is negatively directed
T = 4°K
0.1 msec/cm horizontal

Fig. A.5 – Above threshold laser long pulsed

Table A-I
Diodes Which Lased at 77°K With a Current Pulse of 5 μsec

Diode	Pulse Amplitude (amps)	Repetition Rate (μsec)	Pulse Amplitude (amps)	Repetition Rate (μsec)
H-4	10	380		
H-8	No lasing			
H-13	Bad			
H-16	10	380		
H-17	Bad			
H-18	No lasing			
H-21	Bad			
H-22	No lasing			
H-23	No lasing			
H-24	Bad			
H-25	No lasing			
H-26	8	200		
H-28	11	380		
H-43	6	150		
H-4′	No lasing			
H-27	9	150		
H-30	9	160	Double-sided diodes	
H-32	10	200	below this line	
H-33	7	120	5	110
H-34	Bad		Bad	
H-38	9	150	8	200
H-39	No lasing		4.3	110
H-40	Bad		Bad	
H-42	5	85	6	80
H-44	Bad		Bad	
H-46	7	75	5	100
H-47	6	140	6.5	150
H-48	Bad		Bad	
H-49	7	60	4	50
H-50	5.5	130	5	110
H-51	8	130	7	100
H-54	3	95	8	200
H-55	4.5	50	4	110
H-56	6	200	5	200
H-57	4	90	5	70
H-49 deteriorated				
	8	65	7	80

APPENDIX B

It was hoped that stub tuned matching would be more compatable with this investigation than were the other matching techniques. The method is more readily described by mathematics, thereby yielding the accuracy needed for this investigation. In order to tune the system it was necessary to construct the device shown in Fig. B.1. To determine the response of this transformer it was necessary to terminate it with the correct impedances such that a sweep generator would yield the proper information. To determine what impedance the transformer would see on the laser end, the RX meter was used. It was convenient to construct a 1/4 wave line from the dewar using an extendable line. Measurement showed that the resulting impedance at the output, with a diode bias of 200 ma, was 540Ω. With 540Ω on the diode side and 50Ω on the amplifier side of the transformer, a Textronix RM565 scope and a Jerrold 900 sweep generator were used in conjunction with an HP52452/5255A frequency counter-standard to obtain the response shown in Fig. B.2. The 1-MHz markers make it easy to see that the band pass of the transformer is wide compared to that of the amplifier seen in Fig. B.3. Due to saturation, the transformer and amplifier combination has a variable bandwidth with gain. Figure B.4 shows that the bandwidth of the combination is no less than that of the amplifier, one of the two primary features being sought in a matching device. When the laser was connected to the transformer with a 1/4 wave line, the ¼λ line itself becomes part of the transformer. This degrades the frequency response which now varies from 1.5 to 3 MHz with gain. In addition to having at least a 3-MHz bandwidth it was necessary that the transformer have low loss. Although this transformer had the lowest loss of any that were constructed, it was ~7 dbm, as measured with the sweep generator and a variable attenuator. These results precluded the use of this transformer in the noise measuring system.

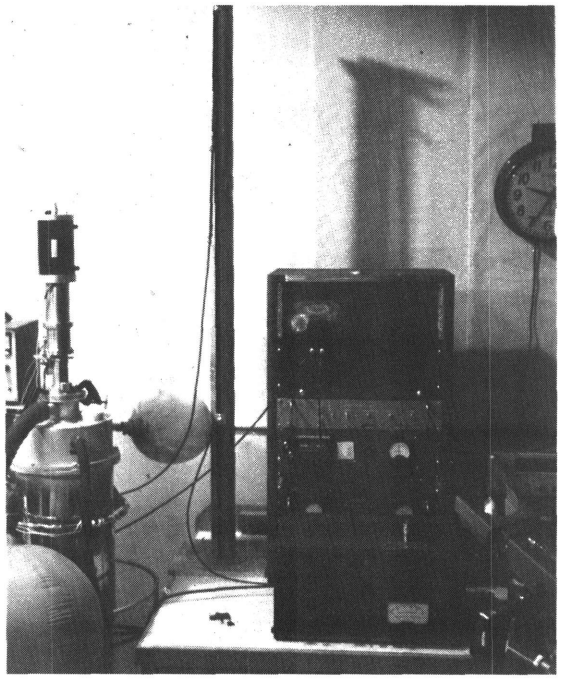

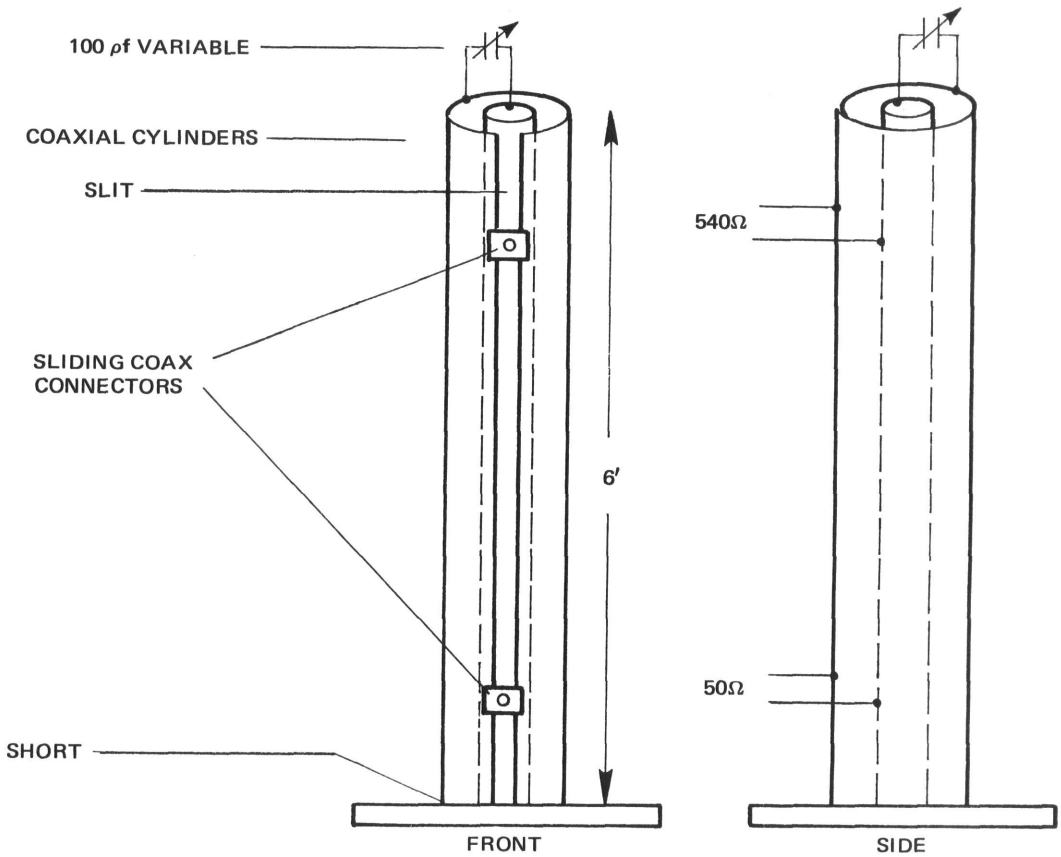

Fig. B.1 – Stub-tuned transformer

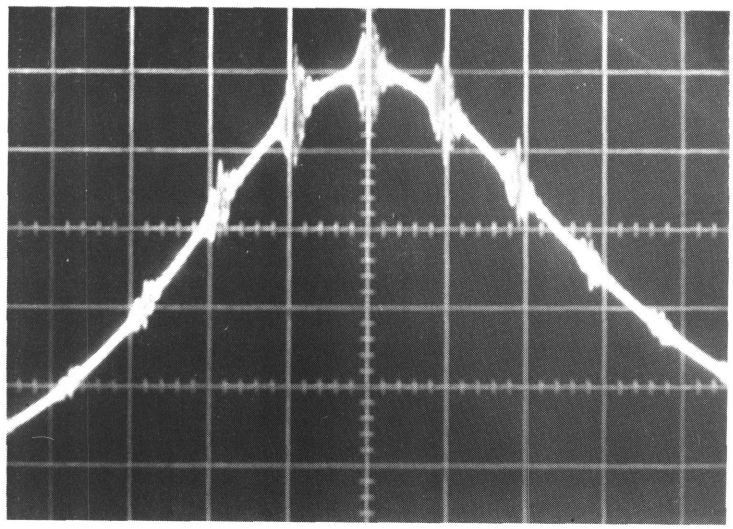

Fig. B.2 – Transformer response, 540Ω:50Ω

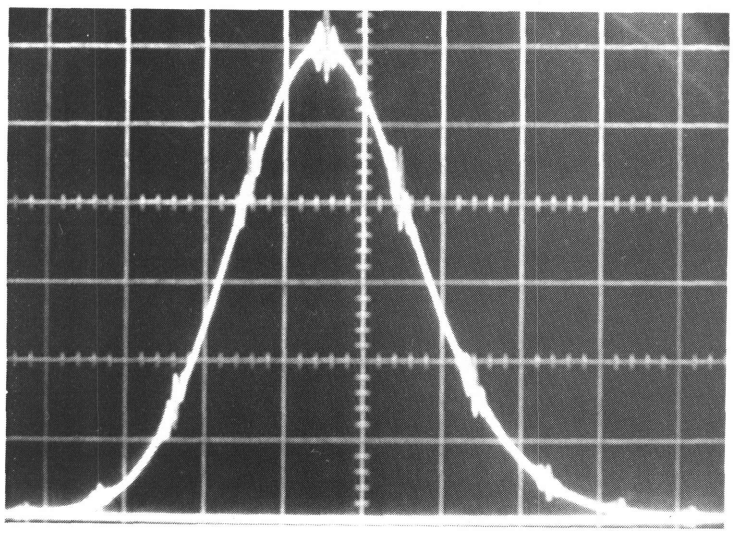

Fig. B.3 – Amplifier response

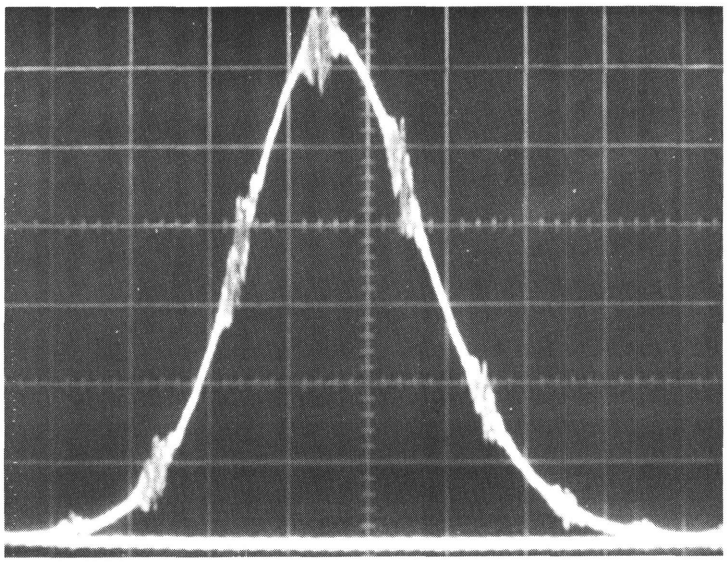

Combined transformer-amplifier response at low gain

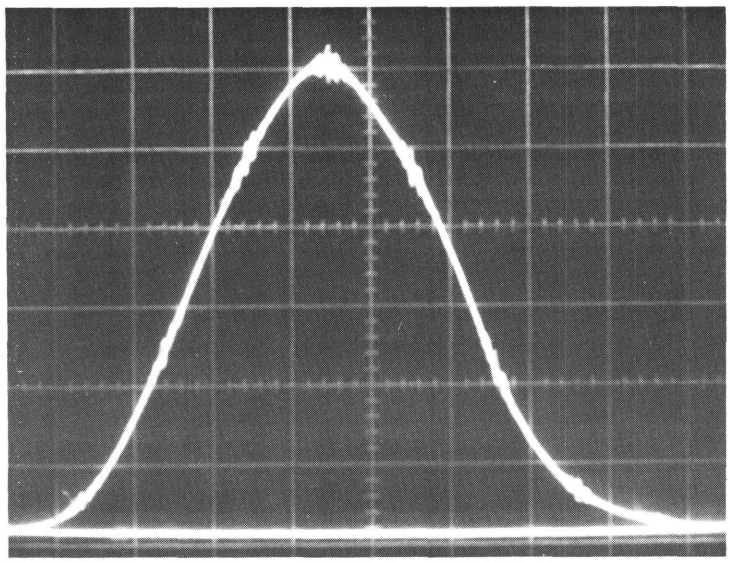

Combined transformer-amplifier response at high gain

Fig. B.4 – Transformer-amplifier response

APPENDIX C

H-31 T = 77°K

I_d (ma)	C_a (dbm)	$(r_d/r_s)^2$	$\overline{i_{dT}^2}/\Delta f$	$\overline{i_{dT}^2}/\Delta f$
100	0.6	–	–	54.67
300	0.7	1.13	51.31	57.98
460	0.8	1.0	61.21	61.21
560	0.9	1.0	64.37	64.37
660	1.0	1.0	67.46	67.46
760	1.1	1.0	70.48	70.48

H-31 T = 4°K

I_d (ma)	C_a (dbm)	Photomult(mv)	$(r_d/r_s)^2$	$\overline{i_{dT}^2}/\Delta f$	$\overline{i_{dT}^2}/\Delta f$
140	0.1	0.6	1.7	21.72	36.92
260	0.2	1.2	–	–	40.64
350	0.3	1.8	1.12	39.52	44.26
420	0.4	2.4	1.0	47.81	47.81
480	0.5	2.9	1.0	51.28	51.28
540	0.6	3.1	1.0	54.67	54.67
595	0.7	3.0	1.0	57.98	57.98
640	0.8	3.0	1.0	61.21	61.21
680	0.9	3.0	1.0	64.37	64.37
730	1.0	2.8	1.0	67.46	67.46
760	1.1	3.0	1.0	70.48	70.48

H-52 T = 4°K Narrow Side

I_d (ma)	C_a (dbm)	$(r_d/r_s)^2$	$\overline{i_{dT}^2}/\Delta f$	$\overline{i_{dT}^2}/\Delta f$
170	0.2			
220	0.3			
245	0.4	1.3	36.78	47.81
265	0.5			
290	0.6			
310	0.7	1.13	51.31	57.98
324	0.8			
340	0.9			
360	1.0	1.12	60.23	67.46
375	1.1			
385	1.2			
400	1.3	1.08	70.66	76.32
435	1.6	1.0	84.58	84.58
455	1.8	1.0	89.78	89.78
480	2.1	1.0	97.14	97.14
500	2.3	1.0	101.77	101.77
551	3.2	1.0	120.18	120.18
600	4.2	1.0	136.62	136.62
650	5.6	1.0	154.11	154.11
700	8.1	1.0	174.24	174.24
735	12.1	1.0	189.80	189.80
760	22.1	1.0	199.07	199.07

H-52 T = 4°K Wide Side

I_d (ma)	C_a (dbm)	$(r_d/r_s)^2$	$\overline{i_{dT}^2}/\Delta f$	$\overline{i_{dT}^2}/\Delta f$
145	0.1	1.7	21.72	36.92
245	0.2	1.3	31.26	40.64
315	0.3	1.13	39.17	44.26
355	0.4	1.12	42.69	47.81
395	0.5	1.08	47.48	51.28
440	0.6		54.67	
465	0.7		57.98	
500	0.8		61.21	
525	0.9		64.37	
545	1.0		67.46	
575	1.1		70.48	
595	1.2		73.43	
620	1.3		76.32	
635	1.4		79.13	
655	1.5		81.89	
675	1.6		84.58	
690	1.7		87.21	
710	1.8		89.78	
725	1.9		92.29	
735	2.0		94.74	
755	2.1		97.14	

H-55 T = 4°K

I_d (ma)	C_a (dbm)	Photomult (mv)	$(r_d/r_s)^2$	$i^2_{dT}/\Delta f$	$i^2_{dT}/\Delta f$
40	.1				
100	.1+	0.7			
125	.1+	1.0			
140	.1+	1.2	1.7	21.72	36.92
160	.1+	1.6			
180	.1+	2.2			
200 Lasing	.1+	2.8–3.4			
220 Lasing	.1++	4.8–6.2			
240 Lasing	.1++	7.0–10.0	1.3	28.4	37.0
520 Lasing	.2		1.0	40.64	40.64
780 Lasing	.3		1.0	44.26	44.26

REFERENCES

1. R. L. Anderson and A. van der Ziel, "On the shot effect of p-n junctions," Trans. IRE, vol. E0-1, Nov. 1952, pp. 20-24.
2. A. van der Ziel, **Noise**, Prentice-Hall, New York, 1954.
3. A. van der Ziel, "Theory of shot noise in junction diodes and junction transistors," Proc. IRE, Nov. 1955, pp. 1639-1646.
4. A. Uhlir, Jr., "High frequency shot noise in **P-N** junctions," Proc. IRE, April 1956, pp. 557-558.
5. N. Guggenbuehl and M. J. O. Strutt, "Theory and experiments on shot noise in semiconductor junction diodes and transistors," Proc. IRE, June 1957, pp. 839-854.
6. A. van der Ziel and A. G. T. Becking, "Theory of junction diode and junction transistor noise," Proc. IRE, March 1958, pp. 589-594.
7. B. Schneider and M. J. O. Strutt, "Theory and experiments on shot noise in silicon **P-N** junction diodes and transistors," Proc. IRE, April 1959, pp. 546-554.
8. M. I. Nathan, "Semiconductor lasers," Proc. IEEE, Oct. 1966, pp. 1276-1290.
9. A. van der Ziel, "Theory of emission noise in lasers," Proc. IEEE, Dec. 1964, p. 1738.
10. J. A. Armstrong and A. W. Smith, "Intensity fluctuations in GaAs laser emission," Physical Review, Oct. 1965, pp. A155-A165.
11. A. W. Smith and J. A. Armstrong, "Intensity noise in multimode GaAs laser emission," IBM Journal, May 1966, pp. 225-232.
12. J. J. Brophy, "Fluctuations in luminescent junctions," Journal of Applied Physics, May 1967, pp. 2465-2469.
13. G. Guekos and M. J. O. Strutt, "Current noise spectra of GaAs laser diodes in the luminescence mode," IEEE Journal of Q.E., Aug. 1968, pp. 502-503.

14. H. Haug, "Population and current noise in semiconductor laser junctions," Zeitschrift für Physik, vol. 206, 1967, pp. 163-176.

15. J. J. Freeman, **Principles of Noise**, John Wiley and Sons, New York, 1958, pp. 111-112.

16. H. R. Raemer and A. B. Reich, "Correlation devices," Electronics, May 22, 1959, pp. 58-60.

17. "Instruction handbook for AIL 74 Automatic Noise Figure Indicator," Airborn Instruments Laboratory, New York, 1961.

18. R. J. Proebsting, "Wavelength stability of GaAs diode lasers," Doctor of Philosophy Thesis, University of Wisconsin, 1967.

19. Private correspondence with persons involved with government and industrial transformer research.

20. F. E. Terman, **Radio Engineers' Handbook**, McGraw-Hill, New York, 1943, pp. 26-172.

21. Private correspondence on the results of this investigation with A. van der Ziel, University of Minnesota.

22. G. Guekos and M. J. O. Strutt, "Correlation between laser emission noise and voltage noise in GaAs cw laser diodes," IEEE Journal of Q.E., Feb. 1969, pp. 129-130.

23. G. Guekos and M. J. O. Strutt, "Laser emission noise and voltage noise of GaAs cw laser diodes," Electron. Letters, vol. 4, 1968, pp. 408-409.

This page intentionally left blank.

Security Classification

DOCUMENT CONTROL DATA - R & D

(Security classification of title, body of abstract and indexing annotation must be entered when the overall report is classified)

1. ORIGINATING ACTIVITY *(Corporate author)* Naval Research Laboratory Washington, D. C. 20390	2a. REPORT SECURITY CLASSIFICATION Unclassified 2b. GROUP

3. REPORT TITLE

ELECTRICAL NOISE IN GaAs DIODE LASERS

4. DESCRIPTIVE NOTES *(Type of report and inclusive dates)*

Final report on one phase of research under the problem. Oct. 68–Jan. 69

5. AUTHOR(S) *(First name, middle initial, last name)*

T. Robert Royt

6. REPORT DATE October 30, 1969	7a. TOTAL NO. OF PAGES 65	7b. NO. OF REFS 23
8a. CONTRACT OR GRANT NO. NRL Problem R06-38 b. PROJECT NO. SS 33-18-11917 c. d.	9a. ORIGINATOR'S REPORT NUMBER(S) NRL Report 6980 9b. OTHER REPORT NO(S) *(Any other numbers that may be assigned this report)*	

10. DISTRIBUTION STATEMENT

This document has been approved for public release and sale; its distribution is unlimited.

11. SUPPLEMENTARY NOTES	12. SPONSORING MILITARY ACTIVITY Department of the Navy (Naval Ship Systems Command), Washington, D.C. 20360

13. ABSTRACT

This investigation makes measurements of the current fluctuations at 30 MHz generated in a GaAs diode during luminescent and lasing operation. For the diodes employed, it is found that thermal noise predominates over other effects. Calculations indicate that this dominance is due to the small junction resistances which occur at helium temperatures. In addition, the line loss in the transmission system was found to limit the measurement system sensitivity.

DD FORM 1 NOV 65 1473 (PAGE 1)

S/N 0101-807-6801

Security Classification

Security Classification

14. KEY WORDS	LINK A ROLE	LINK A WT	LINK B ROLE	LINK B WT	LINK C ROLE	LINK C WT
GaAs diode lasers						
Electrical noise						
Fluctuation theory						
Autocorrelation function						
Impedance transformation						

DD FORM 1 NOV 65 1473 (BACK)
(PAGE 2)

Security Classification